Chemical Geology 670 (2024) 122434

Contents lists available at ScienceDirect

Chemical Geology

journal homepage: www.elsevier.com/locate/chemgeo

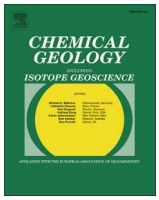

Helium, carbon and nitrogen isotope evidence for slab influence on volcanic gas emissions at Rabaul caldera, Papua New Guinea

B.T. McCormick Kilbride [a,*], P.H. Barry [b], T.P. Fischer [c], G. Holland [a], M. Hudak [d], S. Nowicki [c], C. Ballentine [e], M.D. Fox [f], M. Höhn [a], I. Itikarai [g], M.D. Johnson [f], K. Mulina [g], E.J. Nicholson [h,i]

[a] Department of Earth Sciences, University of Manchester, USA
[b] Marine Chemistry and Geochemistry Department, Woods Hole Oceanographic Institution, USA
[c] Department of Earth and Planetary Sciences, University of New Mexico, USA
[d] Department of Geosciences, Williams College, USA
[e] Department of Earth Sciences, University of Oxford, UK
[f] Division of Biological and Environmental Science and Engineering, King Abdullah University of Science and Technology, Saudi Arabia
[g] Rabaul Volcanological Observatory, Papua New Guinea
[h] Department of Earth Sciences, University College London, UK
[i] Department of Earth Sciences, University of Waikato, New Zealand

ARTICLE INFO

Editor: Claudia Romano

Keywords:
Subduction zone
Volatiles
Volcanic gas
Noble gas
Carbon isotopes
Nitrogen isotopes

ABSTRACT

The chemical and isotopic composition of gases emitted by subduction zone volcanoes can provide insights into the origin of magmatic volatiles. In volcanic arcs, magmatic volatiles can be supplied from the mantle, the subducting slab, or the rocks of the arc crust. Determining the relative contributions of these distinct sources is important for understanding the transfer of volatiles between Earth's interior and exterior reservoirs, which has implications for the physical and chemical evolution of both the mantle and the atmosphere. Each subduction zone has a different recycling efficiency, controlled by the composition of the slab and the pressure-temperature path it experiences upon subduction, and accordingly all volcanic arc emissions can be characterised by their chemical and isotopic compositions. In this study, we analyse the composition of volcanic gases from Rabaul caldera in the New Britain subduction zone, Papua New Guinea, and show that the emissions are substantially influenced by slab recycling of carbon and nitrogen. We find helium emissions are dominated by a mantle contribution, with little influence from the arc crust. Carbon isotopes point towards a mixture of mantle, carbonate and organic sediment-derived contributions, with the dominant input coming from carbonates. This may be of sedimentary origin, seafloor calcareous muds, or altered basalts of the subducting oceanic crust. Nitrogen isotopes also indicate a significant influence of sedimentary nitrogen and, potentially, a contribution from altered ocean crust. Our study is the first comprehensive investigation of volatile sources in the New Britain subduction zone and our results and interpretation are consistent with previous studies of element recycling based on New Britain arc lavas.

1. Introduction

Rabaul is a restless caldera volcano in East New Britain province, Papua New Guinea (PNG, Fig. 1). Since the last caldera forming eruption (667–699 CE), there have been numerous eruptions, of diverse styles, from multiple intra-caldera vents (Bernard and Bouvet de Maisonneuve, 2020; Fabbro et al., 2020; Heming, 1974; McKee et al., 2015; Patia et al., 2017; Wood et al., 1995). The most recent eruptions (1994–2014) were accompanied by substantial outgassing from the caldera's most active cone, Tavurvur (Carn et al., 2016; Global Volcanism Program, 2013; McCormick et al., 2012). Rabaul has been cited as among the highest emitters of volcanic gas into the atmosphere over the past two decades and Tavurvur, where outgassing has been focussed, was ranked seventh worldwide for both SO_2 and CO_2 flux in 2005–2015 (Aiuppa et al., 2019; Carn et al., 2017). Following the cessation of eruptive activity, unrest at Rabaul has dwindled to significantly lower levels, in terms of the intensity of seismicity, ground deformation, vigour of gas emissions, and the temperature and overall abundance of hot springs and fumaroles

* Corresponding author.
E-mail address: brendan.mccormickkilbride@manchester.ac.uk (B.T. McCormick Kilbride).

https://doi.org/10.1016/j.chemgeo.2024.122434
Received 1 March 2024; Received in revised form 26 September 2024; Accepted 30 September 2024
Available online 1 October 2024

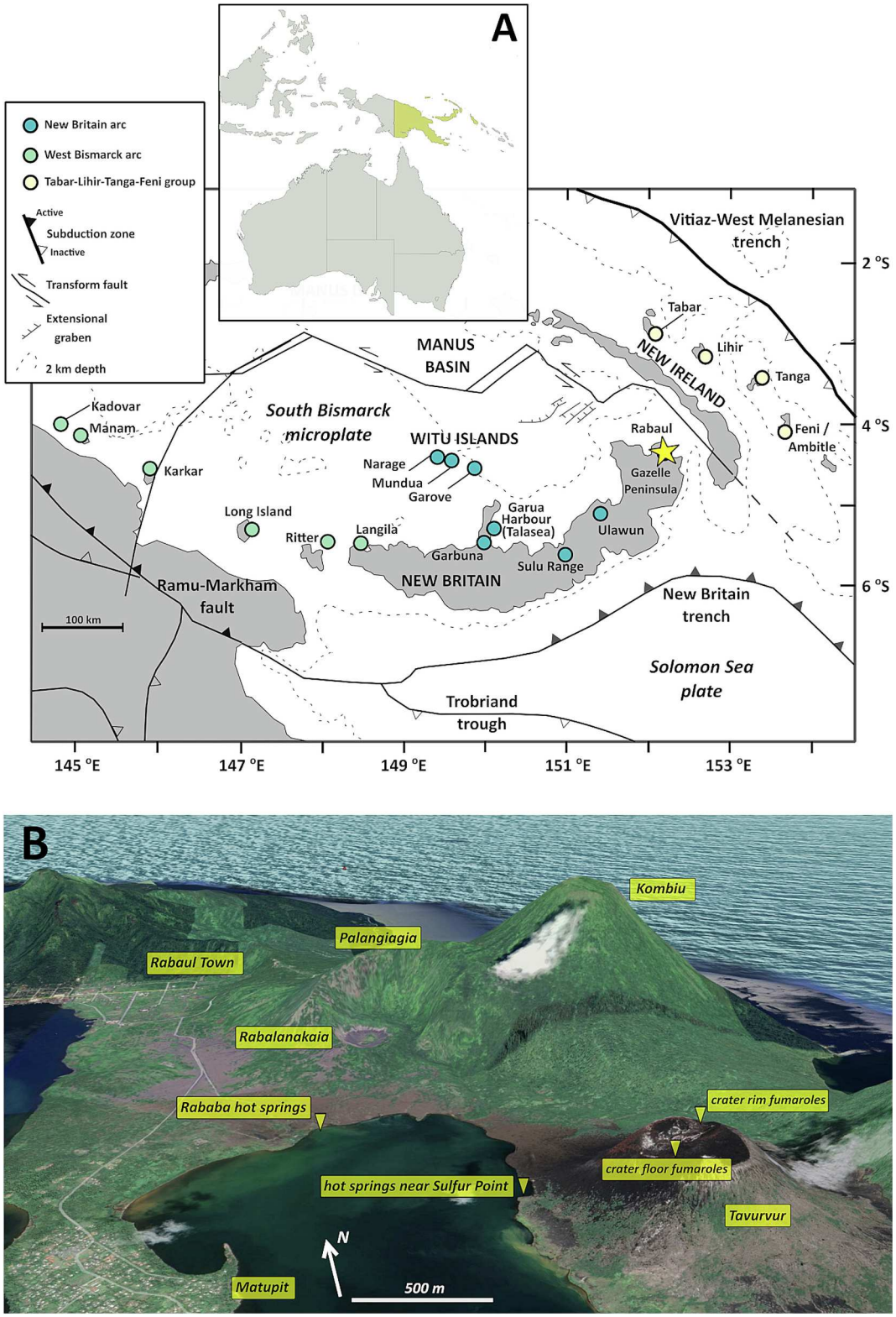

Fig. 1. A. Map of New Britain, highlighting tectonic or geographic features mentioned in the text and selected volcanoes of the West Bismarck, New Britain, and Tabar-Lihir-Tanga-Feni groups. Of the volcanoes shown, all except Tabar, Tanga and Narage have reported Holocene activity (Global Volcanism Program, 2013). Map modified from (Holm et al., 2016; Macpherson et al., 1998). Inset shows location of PNG within Oceania. B. Google Earth image showing Rabaul caldera with major features (urban areas, volcanic edifices, our sampling sites) highlighted.

across the caldera. It remains unclear whether prodigious gas emissions from Rabaul are an inherent characteristic of the volcanic system or a transient feature, given the short history of instrumented monitoring. The chemical and isotopic composition of gas emissions at Rabaul have been little studied (Farley et al., 1995; Sano and Williams, 1996) and we do not know whether, or to what extent, volatiles are supplied to the volcanic system from (i) the nearby subducting Solomon Sea plate or (ii) crustal rocks of the New Britain volcanic arc. Magmatic volatiles play a key role in modulating eruption style and intensity at Rabaul and understanding their origin and abundance is critically important for hazard assessment and risk mitigation (Bernard et al., 2022).

In this contribution, we present geochemical and isotopic data from volcanic gases at Rabaul, collected from Tavurvur crater fumaroles and nearby hot springs in 2016 and 2019. We report the composition of gases in terms of the relative abundance of major (H_2O, CO_2, sulfur) and trace (He, Ar, N_2) chemical species, as well as helium, carbon, nitrogen, argon, krypton and xenon isotopes. These are valuable tracers for determining the relative proportion of volatiles supplied from the mantle and the crust (Barry et al., 2022; Hilton et al., 2002) as well as for assessing the influence of recycled subducting slab phases (Fischer et al., 2002; Halldórsson et al., 2013; Mitchell et al., 2010; Sano and Marty, 1995). On the scale of individual volcanic systems, such information is valuable for understanding magmatic volatile budgets and for interpreting the chemistry of gas emissions. Considering a group of volcanoes, whether within the same arc or in different arcs, we can learn about the variable efficiency of volatile recycling during subduction (where recycling is defined as return flux to the surface) according to differences in the phases present on the slab and the pressure-temperature path experienced by the slab as it sinks (Aiuppa et al., 2019; Hilton et al., 2002; Plank and Manning, 2019). Taken globally, these insights into volatile recycling efficiency during subduction contribute to our understanding of the secular evolution of mantle and atmospheric composition, plate tectonics, environmental change, and planetary habitability (Bekaert et al., 2021; Hilton et al., 2002; Jambon, 1994).

Our understanding of magmatic volatile budgets at Rabaul and of volatile recycling in the wider New Britain subduction zone is at an early stage. In this study, we have characterised the isotopic and chemical composition of fumaroles on the active cone of Tavurvur and hot springs around Rabaul caldera for the first time. Many of our samples are affected by air contamination, potentially due to shallow seawater intrusion or air circulation in the hydrothermal system within the poorly consolidated rocks of the volcanic edifice. Nonetheless, by combining a range of complementary chemical and isotopic tracers, along with a compilation of the available geochemical and isotopic data from whole rock analyses, we have determined the provenance of volatiles at Rabaul. We find a strong mantle influence, based on high $^3He/^4He$ values, and evidence from $\delta^{13}C$ for slab-derived carbonate and organic sediment contributions. Evidence from $\delta^{15}N$ suggests air, sedimentary and minor mantle sources of nitrogen.

2. Geological context

2.1. Tectonic setting

Rabaul is located on the Gazelle Peninsula of New Britain in a complex tectonic setting between the converging Pacific and Australian plates (Holm et al., 2016; Woodhead et al., 1998). The island is built of Eocene-Oligocene volcanic rocks and intrusives, with overlying Miocene limestones and younger volcanics. Modern convergence is accommodated by microplate rotation and subduction of the Solomon Sea plate beneath the Bismarck Sea (Fig. 1). The convergence rate at the New Britain trench is ~9–13 cm yr^{-1} (Holm et al., 2016; Tregoning et al., 2000, 1998; Woodhead et al., 1998). New Britain's Paleogene volcanic and igneous rocks are related to an earlier period of subduction, when the Pacific plate was subducted along the now inactive Vitiaz-West Melanesian trench to the northeast of modern New Ireland (Fig. 1). Subduction along this margin ended around 26–20 Ma, possibly caused by the docking of the Ontong-Java plateau with the trench. The pause between these two phases of arc magmatism permitted the development of platform carbonates, in the Gazelle Peninsula represented by the Yalam Formation (Lindley, 2006; Madsen and Lindley, 1994).

The New Britain subduction zone is typical of intra-oceanic convergent margins (Leat and Larter, 2003). The Solomon Sea slab dips ~70° northwards beneath the Gazelle Peninsula, steepening to subvertical towards its western end at 149° E (Gong et al., 2023; Zhang et al., 2023). Rabaul is ~148 km above the slab (Syracuse and Abers, 2006). The subducting crust age is 24–44 Ma based on heat flow measurements (Joshima and Honza, 1986) and 28–34 Ma based on magnetic lineations (Joshima et al., 1986). There are no ocean drill cores of the Solomon Sea, but samples of seafloor sediments and basalts obtained by dredges and freefall grabs from the R.V. *Natsushima* in 1983–4 may represent the subducting slab lithologies. The sediments are hemipelagic lower bathyal deposits comprising claystones and tuffaceous calcareous muds (Crook, 1986). The volcanic samples are variably altered ferrobasalts, both quench-textured lavas and devitrified hyaloclastites (Davies and Price, 1986). The major and trace element chemistry and Sr-Nd-Pb isotopic composition of these rocks was reported by Woodhead et al. (1998). Sediments sampled from the upper New Britain trench wall comprise a complex suite of limestones, glauconite-bearing sediments, and arenites and rudites derived from both volcanic rocks and carbonates (Crook, 1986). At the western end of the trench, there is a 2.5 km-thick accretionary prism which is absent at the eastern end, closest to Rabaul (Honza et al., 1989). It remains unclear whether the uneven distribution of sediment in the New Britain trench is a consequence of lateral sediment transport caused by oblique plate convergence, greater debris infill at the western end due to proximity to the Western Bismarck arc and Australian continent collision zone, efficient subduction of sediment at the eastern end of the trench, or an eastward increase in tectonic erosion of the forearc crust (Bernstein-Taylor et al., 1992; Galewsky and Silver, 1997; Honza et al., 1989; Malatesta et al., 2013).

2.2. Eruptive history of Rabaul

Volcanism on the Gazelle Peninsula dates from the Lower to Middle Pleistocene and is distributed across four major centres, the Varzin Depression, the Vanakunau Basin, the submarine Tavui caldera and Rabaul, the youngest and most active (Hohl et al., 2022; McKee, 2015; Nairn et al., 1995). The oldest dated deposits at Rabaul (~0.5 Ma) are associated with three basaltic stratovolcanoes, Tovanumbatir, Kombiu and Turangunan, adjacent to the modern caldera (McKee and Duncan, 2016). Since 0.125 Ma, nine ignimbrite-forming eruptions have occurred, most recently the Rabaul Pyroclastics event in 667–699 CE, which deposited an 11 km^3 ignimbrite and formed a 6 × 8 km caldera (McKee et al., 2015; Nairn et al., 1995). Historical eruptions have occurred at multiple vents within the caldera (Tavurvur, Vulcan, Rabalanakaia, Sulfur Creek, Palangiagia), including events in 1878, 1937 and 1994 where Vulcan and Tavurvur erupted simultaneously. The post-caldera eruptions have exhibited lava flows, violent Strombolian behaviour, and Vulcanian to sub-Plinian blasts, with the diversity in eruption dynamics attributed to variations in magma ascent rate (Bernard and Bouvet de Maisonneuve, 2020). Caldera-forming eruptions are of dacitic composition while post-caldera eruption products range from basaltic andesite to trachydacite (58–64 wt% SiO_2) (Bernard and Bouvet de Maisonneuve, 2020; Fabbro et al., 2020; Nairn et al., 1995). Intermediate magmas at Rabaul apparently result from the mingling and mixing of recharging basalts and resident dacites (Bouvet de Maisonneuve et al., 2015; Patia et al., 2017). There has been no eruption at Rabaul since August 2014.

2.3. Previous work on magma and volatile sources at Rabaul

The mantle wedge beneath New Britain, of Indian MORB affinity

based on whole-rock Pb isotopes, is exceptionally depleted in high field strength elements (HFSE), a consequence of prior melting in the back arc, i.e., Manus Basin (Woodhead et al., 1998). Post-Miocene New Britain volcanics are enriched in fluid mobile elements (e.g., Ba/La, Sr/Nd), resulting from slab fluids infiltrating the mantle wedge (DePaolo and Johnson, 1979; Johnson, 1979). Based on Sr-Nd-Pb isotopes, high Sr/Nd and low Th/Yb ratios, Woodhead et al. (1998) described New Britain volcanics as an end-member suite among global arcs, bearing a strong influence of hydrous fluids derived from altered basaltic crust with relatively minor influence of recycled sediments. This interpretation was previously advanced on the basis of lava B/Be ratios (Morris et al., 1990). New Britain arc volcanoes lie over a remarkably wide range in depth to the slab, from ~100 km at the volcanic front to ~600 km at the Witu Islands (Johnson, 1979; Woodhead and Johnson, 1993). Tracers of slab fluid in the erupted lavas (e.g., Ba/La, Sr/Nd, $^{206}Pb/^{204}Pb$, Eu anomaly) diminish from south to north across the arc, suggesting a decrease in fluid influence with increasing depth to slab. This trend is convolved with increasing HFSE concentration, reflecting a decrease in partial melting, also correlated with depth to slab (DePaolo and Johnson, 1979; Woodhead et al., 1998; Woodhead and Johnson, 1993). Rabaul is not included in the data presented by Woodhead et al. (1998), though the authors note that limited Sr—Pb isotopic analyses of 1994 Vulcan and Tavurvur andesites are notably more radiogenic than other New Britain rocks (Johnson et al., 1995) and that this may be a consequence of 'paleo-enrichment' of the mantle wedge, related to the earlier subduction of the Pacific plate (see section 2.1). More recent work (Hohl et al., 2022), argues for the influence of both slab-derived fluids and slab sediment-derived melts on the mantle beneath Rabaul, based on trace element and Sr-Nd-Hf isotope analyses of 'inner caldera' (post-1400 B.P. eruptions of Tavurvur, Vulcan, Rabalanakaia, Sulfur Creek) and outer caldera (undated rocks from neighbouring mafic stratovolcanoes, e.g., Kombiu) deposits. Titanium isotope heterogeneities in basaltic rocks from New Britain arc volcanoes, though not Rabaul, have been suggested to reflect the influence of hydrous slab partial melts on arc magma generation (Klaver et al., 2024).

Studies of gas emissions from Rabaul and other PNG volcanoes have largely focussed on determining SO_2 and CO_2 flux, using drone-based sensing (Galle et al., 2021; Liu et al., 2020; McCormick Kilbride et al., 2023), ground-based remote sensing (Andres and Kasgnoc, 1998; McGonigle et al., 2004) or satellite observations (Carn et al., 2017; McCormick et al., 2012). These data show that PNG volcanoes (specifically Rabaul, Manam and Bagana) are globally important sources of both SO_2 and CO_2 (Aiuppa et al., 2019; Carn et al., 2017; Fischer et al., 2019). Analyses of gas chemistry are more restricted. Soil CO_2 emissions at Rabaul were sporadically monitored in the 1990s (Global Volcanism Program, 1997a, 1997b, 1995). Otherwise, there are two measurements of helium isotopes in hot spring gases (Farley et al., 1995) and two measurements of helium and carbon isotopes in gas samples from Tavurvur and Rabalanakaia (Sano and Williams, 1996). The helium isotopes range from 5.7 to 8.6 R/R_A, where R is $^3He/^4He$ ratio in the sample and R_A is the ratio in air, indicating a predominantly mantle-derived helium with little crustal input. The carbon isotopes ($\delta^{13}C$) range from −2.55 to −2.80 ‰ versus Pee Dee Belemnite, consistent with mixing between carbonate and mantle-derived carbon. Recent global compilations of arc outgassing have suggested that the high carbon fluxes from PNG volcanoes are due to efficient recycling of subducted carbon, though no distinction is made between the tectonically and geochemically distinct West Bismarck, New Britain and Bougainville arcs in these studies (Aiuppa et al., 2019, 2017; Plank and Manning, 2019). In contrast, other work has argued for remobilized crustal carbonate as the main source of volcanic CO_2 in PNG (Mason et al., 2017). Here, our aim is to discriminate between these scenarios, and moreover to determine the influence of sediment recycling on Rabaul gas emissions.

3. Methods

3.1. Sampling methods

We sampled multiple sites of gas emissions at Rabaul across two field expeditions, in September 2016 and May 2019. In 2016, we collected gas samples from a fumarole at the base of Tavurvur crater, from hot springs on the beach north of Tavurvur towards Sulfur Point, and from hot springs at Rababa (Fig. 1b). During this fieldwork, we also collected gases from fumaroles at the summit of Garbuna volcano, hot springs near Silanga village close to the Sulu Range, and hot springs from Pangalu village close to the Garua Harbour/Talasea volcanic field (Fig. 1a). In 2019, we sampled fumaroles on the northeast rim of Tavurvur and re-sampled Rababa hot springs (Fig. 1b). In 2024, during a separate field campaign, we collected gases from bubbling submarine hot springs (1–2 m water depth) offshore of Narage volcano, Witu Islands (Fig. 1a).

We collected fumarolic gases at all sites by inserting a titanium tube into the fumarole and connected this tube to our sampling line, composed of a Giggenbach bottle and multiple copper tubes connected in series using silicon tubing. The 2019 Giggenbach bottle was an evacuated glass flask containing 5 M NaOH solution (Broadley et al., 2020; Giggenbach, 1975; Giggenbach and Goguel, 1989). In 2016, the Giggenbach bottle was evacuated, but did not contain any NaOH solution.

We collected all hot spring samples by placing an inverted plastic funnel over a persistent bubbling area, securely immersing the funnel in the hot spring pool, and connecting it to the Giggenbach bottle and copper tubes with silicon tubing (Barry et al., 2022). At all sites, we allowed the line to be flushed with gas for at least 30 min prior to collecting our samples. At the fumarole site and the bubbling springs we also collected gas samples into Tedlar bags for carbon isotopic analyses.

We sampled gases from the Tavurvur crater floor fumaroles in 2019 by means of an uncrewed aerial system (UAS), comprised of a multi-rotor DJI Phantom airframe equipped with a Tedlar gas bag sampling apparatus (Galle et al., 2021; Liu et al., 2020). We determined that the aircraft was in the plume by visual observations and triggered sample capture by means of a set timer.

3.2. Analytical methods

Our samples have been analysed in multiple laboratories in several institutions: the University of Oxford (UO), the University of Manchester (UM, both UK), Woods Hole Oceanographic Institution (WHOI) and the University of New Mexico (UNM, both USA).

3.2.1. Gas chemistry

We analysed headspace gases from the Giggenbach bottles using a combination of gas chromatography and quadrupole mass spectrometry. Dissolved gases from the Giggenbach bottles were analysed using wet chemical techniques and ion chromatography. The analytical procedures have been recently described (Ilanko et al., 2019; Lee et al., 2017). In short, the gas chromatograph with a Discharge Ionization Detector and helium carrier gas was used to determine N_2, $Ar + O_2$, CO_2, CO, CH_4 and H_2 (analytical errors <2 %) and the quadrupole was used to quantify Ar, O_2, He, and N_2 (analytical errors <1 %). The NaOH solution was analysed for CO_2 by alkalinity titration. Sulfur species were analysed by ion chromatography and alkaline iodine titration. Chlorine and fluorine were analysed by ion chromatography. The water content of the samples was determined by difference in weight of the sample bottles before and after collection.

3.2.2. Helium isotopes

Our noble gas analyses followed similar procedures between labs, whether at UO, UM or WHOI (Barry et al., 2022, 2016). At UO, the instruments were an SFT and an ARGUS, at UM a modified VG5400 with

upgraded electronics, and at WHOI a Nu Noblesse. We connected copper tubes to the respective extraction lines using an O-ring connection and released small volumes (*2*–20 cm^3) of gas sample into the clean-up lines. We removed reactive gases using a chemical procedure, exposing the sample to a heated titanium sponge, and then passed the gases through hot and cold getters. We then passed a small aliquot of cleaned gas into a cryogenic trap, which allowed separation of each noble gas. The noble gases measured varied between labs and samples. At UO and WHOI (during 2024 analyses), we measured all stable noble gas isotopes, whereas at WHOI in 2019, we only measured He isotopes and $^4He/^{20}Ne$. We were unable to measure Ne isotopes at UM, hence the lack of $^4He/^{20}Ne$ data for these samples. Given the $^{40}Ar/^{36}Ar$ is very close to air, we could assume an air $^{20}Ne/^{22}Ne$ and $^4He/^{20}Ne$ for most samples. We estimate uncertainties of $\leq$5 % for helium isotopes and $\leq$ 3 % for neon and argon isotopes.

3.2.3. Carbon isotopes

We analysed the Tedlar bag samples (collected in 2019) and Giggenbach bottle samples (collected in 2016) for carbon isotopes using a Delta-Ray Infrared Isotope analyser (Fischer and Lopez, 2016; Galle et al., 2021; Liu et al., 2020). We set up the Delta Ray instrument at Rabaul Hotel, in Rabaul Town (Fig. 1b). The CO_2-free air carrier gas was produced on-site by passing air, pressurized in a tank, through Sulfulime absorbent. The calibration gas was pure CO_2 obtained from a company in PNG. We did not know the $\delta^{13}C$ value of the calibration gas at the time of our analyses in Rabaul, so we collected a sample of this gas and analysed it on the Delta Ray at the University of New Mexico after our return and then retroactively corrected the values obtained during the fieldwork.

3.2.4. Nitrogen isotopes

We performed nitrogen isotope measurements on gas splits from copper tubes. In brief, our fumarole and hot spring gas samples were purified on a specially designed N gas extraction vacuum line (Barry et al., 2012) and analysed for nitrogen isotopes on the Nu Noblesse at WHOI (Bekaert et al., 2024). We placed a third stainless steel clamp on each tube approximately one-half inch from one of the original clamps to subsample an aliquot of the gas in each tube. We connected copper tubes to the extraction line with VCR fittings and pumped down to $<1 \times 10^{-7}$ Torr. Once sufficient vacuum was achieved, we removed the exterior clamp to inlet the aliquot of gas. We froze out condensable gases (mainly CO_2 and H_2O) on a cold finger using liquid nitrogen. The non-condensable gases were expanded into the extraction line and diluted until the sample pressure was low enough to be measured. We then exposed the gas to a Pt furnace at 1000 °C and a CuO furnace that was heated from 450 °C to 850 °C, held for 15 min to covert CO to CO_2, and step cooled back to 450 °C over 30 min. A second cold finger with liquid nitrogen was used to freeze down the CO_2. Once the CuO furnace had cooled to its initial temperatures and CO conversion was complete, we passed an aliquot of the gas into the mass spectrometer for analysis and typically performed each analysis in triplicate. We ran line blanks prior to the analysis (typically <1 %) to use for correction and an air standard following the analysis; the size of the standard is calibrated to match the size of the sample. We applied a linearity correction to match sample signal sizes against air standards signal sizes (Bekaert et al., 2024).

4. Results

The gas compositions (Fig. 2) of our fumarole and hot spring gas samples are reported in Table 1. The helium (Fig. 3) and carbon (Fig. 4) isotopic composition and relative abundance ratios (Fig. 5) are reported in Table 2, along with our estimates of mantle- and slab-derived influences (after Sano and Marty, 1995). In Table 4, we report the nitrogen isotopic composition (Fig. 6) of our samples and independent estimates of mantle- and slab-derived influences (after Sano et al., 2001).

4.1. Gas chemistry

Samples from the 2016 field expedition were collected without NaOH solution in the Giggenbach bottles, so we could not measure H_2O, sulfur or halogen species in these gases. Samples collected in 2019 were dominated by H_2O (678 to 967 mmol/mol in Tavurvur fumaroles, 773

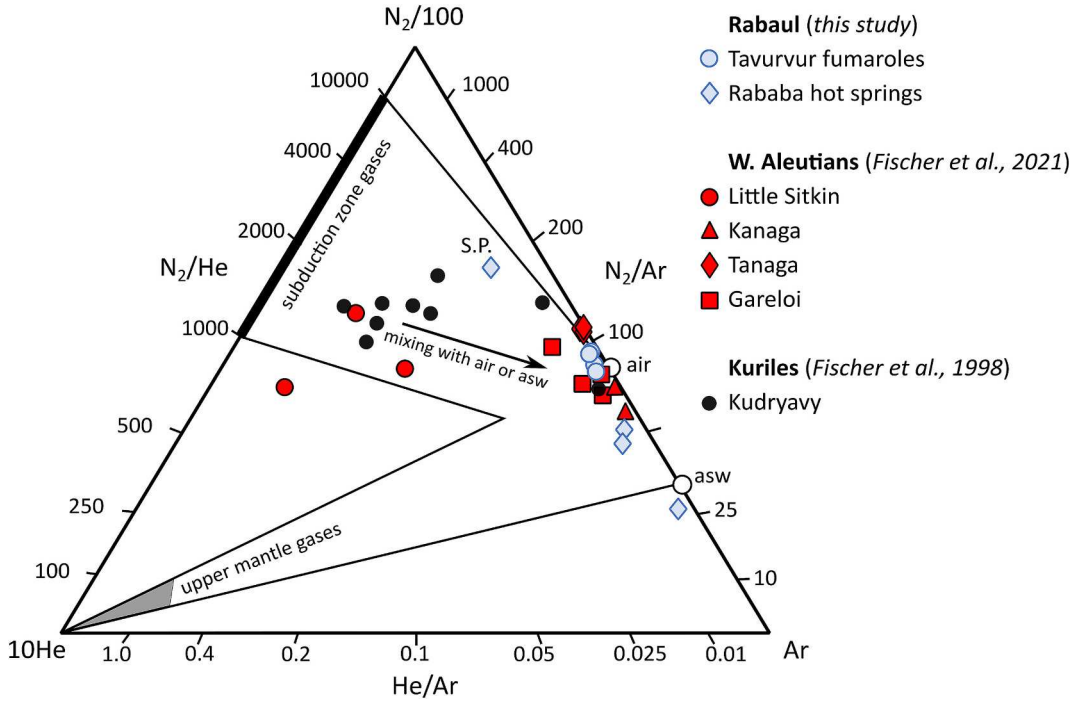

Fig. 2. Ternary diagram showing relative molecular nitrogen, helium and argon (N_2-He-Ar) compositions of fumarole and hot spring gas samples from this study, to highlight magmatic versus air and ASW contributions (Giggenbach, 1980). Also shown are gas data from two other Pacific rim subduction zones (Fischer et al., 2021, 1998).

Table 1
Gas chemistry from fumarole and hot spring gases sampled at Rabaul. Data from 2019 campaign are reported as mmol/mol since we sampled with caustic solution in Giggenbach bottle and could isolate H_2O. Data from 2016 are reported as molar percent dry gas. Concentrations cannot be directly compared across these two campaigns, though N_2/Ar, N_2/He and He/Ar ratios can be. 'nd' signifies not detected.

Site	Sample ID	T (°C)	H_2O	CO_2	St	SO_2	H_2S	HCl	HF	He	H_2	Ar	O_2	N_2	CH_4	CO	N_2/Ar	N_2/He	He/Ar
2019																			
Tavurvur rimfumarole	RB-19-1b	97	967	18.3	3.02	1.99	1.02	0.13	nd	0.00020	0.217	0.181	0.001	11.3	0.00070	nd	62	55,780	0.001
Tavurvur rim fumarole	RB-19-6a	98	678	13.8	2.43	2.1	0.33	0.06	nd	0.00007	0.165	0.085	<0.001	5.35	0.00051	nd	63	77,835	0.001
Rababa hot spring	RB-19-3a	75	773	222.0	1.13	0.06	1.06	0.43	0.07	0.00037	0.001	0.129	0.029	3.57	0.02741	nd	28	9596	0.003
2016																			
Tavurvur floor fumarole	Tav-2B	100		0.33						0.0014	nd	0.850	19.2	79.6	nd	nd	94	56,872	0.002
Tavurvur floor fumarole	Tav-2 A	140		0.45						0.0018	0.017	0.868	19.97	78.7	nd	nd	91	43,720	0.002
Rababa hot spring	RB-HS-1	78		86.6						0.0011	nd	0.219	0.41	12.3	0.521	nd	56	11,155	0.005
Rababa hot spring	RB-HS-3	78		72.9						0.0035	nd	0.497	1.03	25.4	0.083	nd	51	7267	0.007
Hot spring near Sulfur Pt.	RB-HS-2	82		71.60						0.0034	nd	0.128	1.07	27.2	0.046	nd	213	7986	0.026
MORB																	152 ± 58	48 ± 6	2
ASW																	40	150,000	0.0005

mmol/mol in Rababa hot spring gases) with minor CO_2 (13 to 18 mmol/mol in fumaroles and 222 mmol/mol in hot spring gases), and total S (S_t) (0.33 to 2.1 mmol/mol SO_2 and 0.33 to 2.10 mmol/mol H_2S in fumaroles, 0.06 mmol/mol SO_2 and 1.06 mmol/mol H_2S in hot spring gases). CO_2/S_t in the fumarole gases collected in 2019 range from 5.7 to 6.1, slightly higher than what was measured by a 2016 measurement by a MultiGAS instrument in Tavurvur's crater (2.6–2.8, Galle et al., 2021).

Gas samples exhibit high N_2/He, characteristic of volcanic arc gases worldwide, and a wide range in He/Ar and N_2/Ar because of variable mixing between magmatic gases and air or air-saturated water (ASW), which is common in low-temperature arc emissions elsewhere (e.g., the western Aleutians, Fig. 2, Fischer et al., 2021). Air and ASW have N_2/Ar of 83 and 40 respectively (Fischer et al., 1998). The influence of ASW, potentially scrubbing sulfur, is also consistent with the higher CO_2/S_t ratios measured in our Giggenbach bottle samples compared to ratios based on MultiGAS measurements made on the crater floor (Galle et al., 2021). Our samples exhibit high degrees of air or ASW contamination, evidenced by N_2/Ar < 100 and He/Ar < 0.01. High temperature arc gases of pristine magmatic composition (e.g., Kudryavy volcano in the Kuriles, Fischer et al., 1998) tend to have N_2/Ar >100, higher He/Ar, and lower N_2/He; both N_2 and Ar excesses in volcanic gases can be attributed to air contamination during sampling (Giggenbach, 1980).

4.2. Helium isotopes

We have determined the helium isotope composition of 14 fumarole and hot spring gas samples from Rabaul (Fig. 3, Table 2), reported as R/R_A values ($R = {}^3He/{}^4He$ in sample, R_A = atmospheric ${}^3He/{}^4He = 1.39 \times 10^{-6}$). Fumarole gases collected from Tavurvur's crater floor and rim range from 0.92 to 2.70 R_A, while hot spring gases collected from Rababa range from 5.62 to 6.47 R_A, and hot spring gases collected near to Sulfur Point were 3.3 R_A. Fig. 3 also shows helium isotope measurements from volcanic and geothermal gases we sampled elsewhere in New Britain. We also plot helium isotope data from hot springs in Rabaul caldera, fumaroles from the Witu Islands, and various geothermal and fumarolic gases sampled across the nearby Tabar-Lihir-Tanga-Feni (TLTF) group (Craig and Poreda, 1987; Farley et al., 1995). Our helium isotope data from Rabaul hot springs overlap with those of Farley et al. (1995) and Sano and Williams (1996), excluding the Tavurvur sample from the latter study which has R/R_A of 8.6. Our samples from elsewhere in New Britain (Sulu, Talasea, Garbuna) record slightly higher He isotope values with respect to Rabaul. Many of the TLTF gases and the Witu Islands gases approach the MORB range, i.e., ~8 ± 1 R_A (Hilton et al., 2002).

For seven of our samples (Table 2), we use the ${}^4He/{}^{20}Ne$ value to apply an atmospheric correction, assuming that ${}^{20}Ne$ is derived from air (${}^4He/{}^{20}Ne = 0.32$) or ASW (${}^4He/{}^{20}Ne = 0.26$ at 15 °C) (Hilton, 1996; Ozima and Podosek, 2002). This allows us to calculate an atmospheric He value and subtract it from our measured ${}^3He/{}^4He$. Our sample collected on the floor of Tavurvur crater has ${}^4He/{}^{20}Ne$ very close to ASW, suggesting substantial atmospheric contamination, while our remaining samples (Sulfur Point and Rababa hot springs at Rabaul, plus our samples from elsewhere in New Britain) have significantly higher ${}^4He/{}^{20}Ne$, suggesting lesser atmospheric contributions (Fig. 3b). Our correction is based on the methods of (Hilton, 1996), using 'X-values' to correct helium isotope ratios for atmospheric influence. The X-value of a gas sample is defined as:

$$(X)_{gas} = \left({}^4He/{}^{20}Ne\right)_{measured} \Big/ \left({}^4He/{}^{20}Ne\right)_{air}.$$

where $({}^4He/{}^{20}Ne)_{measured}$ is the measured ratio and $({}^4He/{}^{20}Ne)_{air}$ is the value of air, 0.32.

We can then combine our X-values with measured helium isotope values (R/R_A) to calculate atmospheric corrected values (R_C/R_A):

$$R_C/R_A = (R/R_A \times X)–1)/(X–1).$$

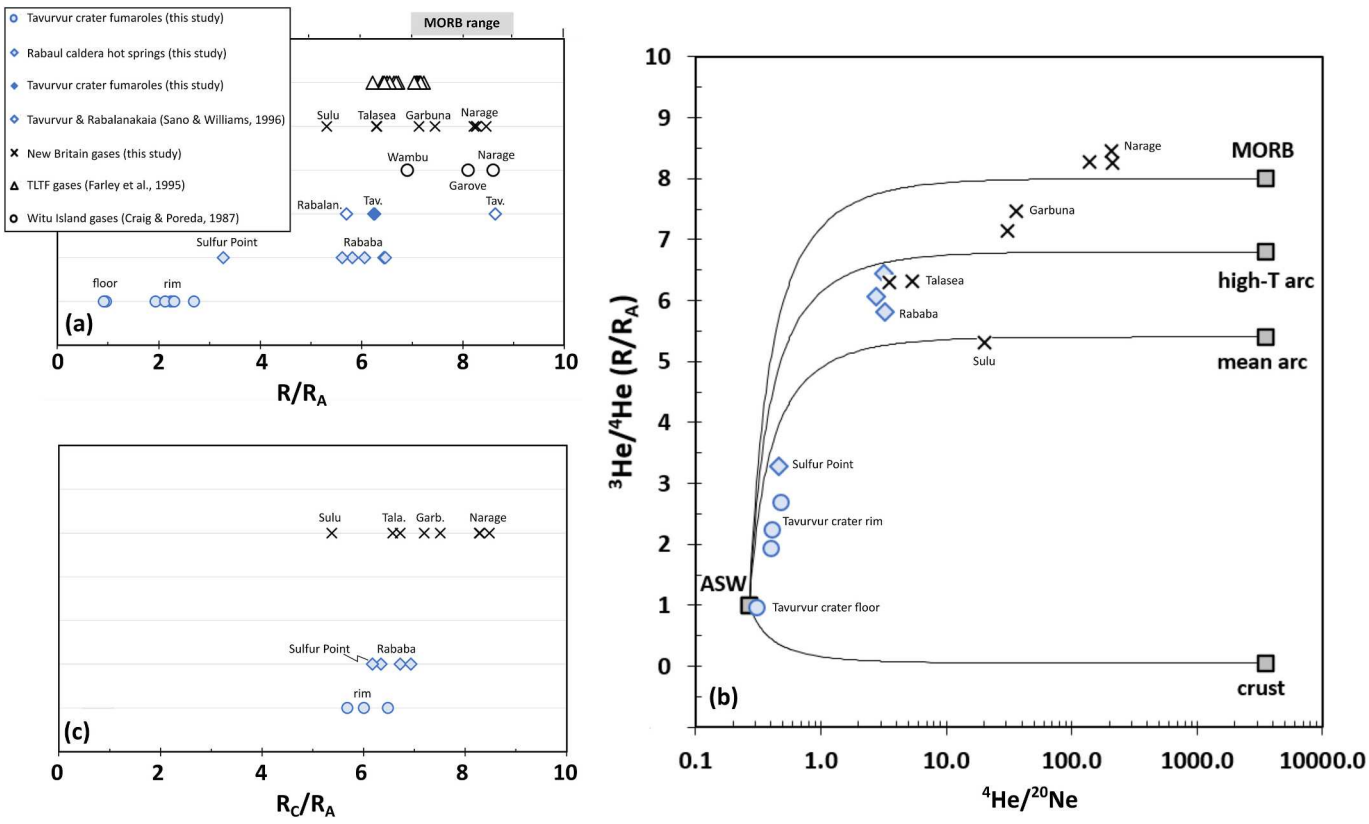

Fig. 3. (a) Helium isotopes measured in fumarole and hot spring gases from Rabaul (this study, Farley et al., 1995; Sano and Williams, 1996), and other volcanoes on New Britain and neighbouring islands (Craig and Poreda, 1987; Farley et al., 1995); (b) the same data plotted versus $^{4}He/^{20}Ne$ along with calculated binary mixing lines between air-saturated water (ASW) and crustal and mantle endmember compositions (Barry et al., 2021; Hilton et al., 2002; Kagoshima et al., 2015); (c) air-corrected helium isotopes for our new Rabaul and New Britain samples.

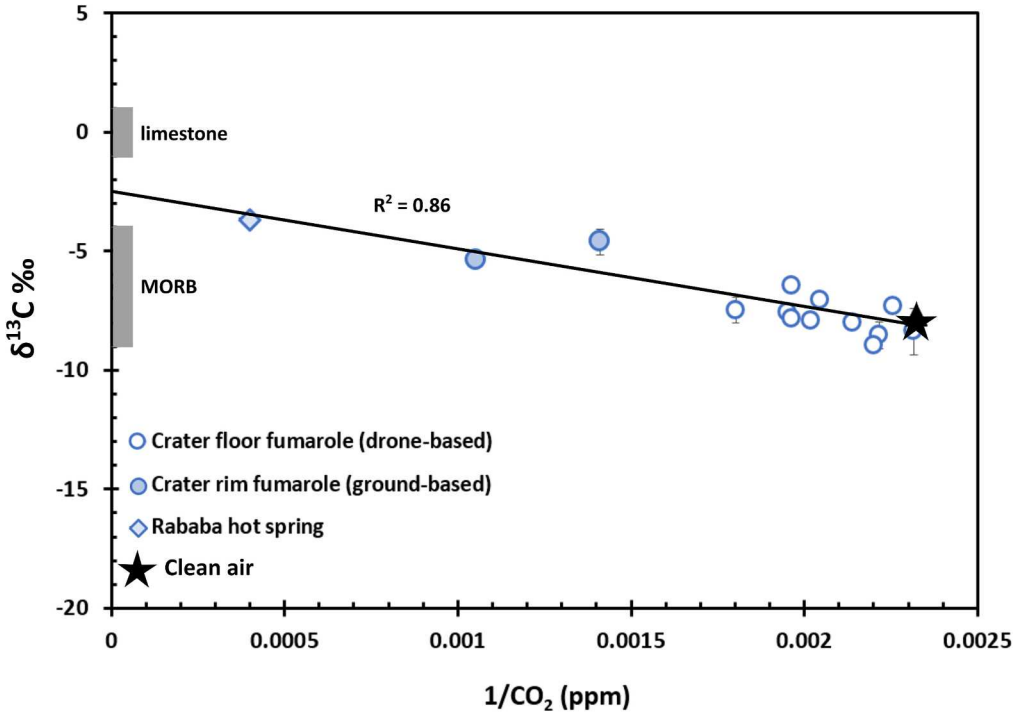

Fig. 4. Relationship between carbon concentration and $\delta^{13}C$ for fumarole and hot spring gases at Rabaul. The typical $\delta^{13}C$ range for reference endmembers are also shown: limestone (subducted marine carbonate, $\delta^{13}C \sim 0$ ‰) and MORB (upper mantle material, $\delta^{13}C \sim -6.5 \pm 2.5$). The black line indicates a mixing line projected from ambient air through the composition of gases sampled from Tavurvur crater floor and rim fumaroles and Rababa hot springs.

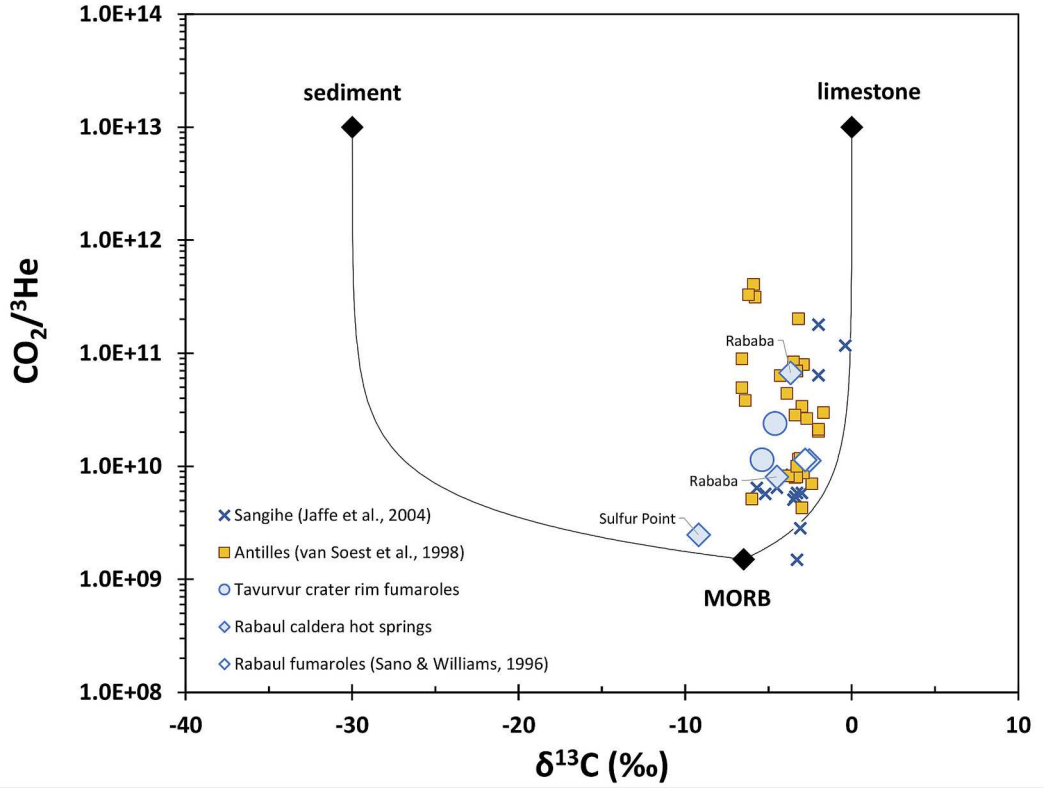

Fig. 5. Three component mixing diagram between $CO_2/^3He$ and $\delta^{13}C$ (CO_2), after (Sano and Marty, 1995). We show new data from Rabaul (Table 2), comprising caldera hot springs and Tavurvur crater fumaroles, previous measurements from Rabaul (Tavurvur and Rabalanakaia) made in 1996 (Sano and Williams, 1996) and published data from two other intra-oceanic arc settings, Sangihe (Jaffe et al., 2004) and the Antilles (van Soest et al., 1998). Model end-members of mid-ocean ridge basalt (MORB), marine limestone (including slab carbonate) and organic sediment are also shown (Sano and Marty, 1995; Sano and Williams, 1996). Black lines show mixing among the end-members.

where R_C/R_A is reported relative to air ($= 1.39 \times 10^{-6}$).

Our samples from Tavurvur rim fumaroles and Rababa and Sulfur Point hot springs show air-corrected He isotope (R_C/R_A) values ranging from 5.7 to 6.9 R_A (Table 2, Fig. 3b). Tavurvur samples show greater air contamination than the hot spring samples and thus the air-correction is significantly larger. As a result, we suggest caution when interpreting these data. Interestingly, air-corrected $^3He/^4He$ (R_C/R_A) values are quite consistent (5.7, 6.0, 6.5 R_A) between the three Tavurvur crater rim samples and these data agree well with air-corrected He isotope data from the nearby Rababa hot springs). We consider the least air contaminated sample of Rababa hot spring, air-corrected He isotope (R_C/R_A) value of 6.7 R_A, as the most representative value of the Rabaul magmatic system. These helium isotope values are below the canonical range for upper mantle helium (8 ± 1 R_A) and high above the range associated with radiogenic (i.e., crustal) helium, 0.05 R_A (Andrews, 1985), suggesting that all samples are a mixture of mantle and radiogenic sources, i.e., the data are bounded by binary mixing curves defining mixtures of air and upper mantle helium, and air and radiogenic helium (Fig. 3b). With regards to helium isotope values in volcanic arcs globally, our Rabaul samples are consistent with the average high temperature fumaroles in volcanic arcs globally of 6.8 R_A (Kagoshima et al., 2015) and within the overall average range of gases emitted from fumaroles and hot springs of arc volcanoes of 5.4 ± 1.9 R_A (Hilton et al., 2002) (Fig. 3b). The Silanga hot springs, near to the Sulu Range volcanoes, have arc-like He isotopes, 5.4 R_A (Fig. 3, Table 2). The Garua Harbour (Talasea) hot springs and Garbuna fumaroles fall in the high-temperature arc range, with 6.6–7.5 R_A. The submarine hot spring samples from Narage volcano fall in the MORB range, with 8.3–8.5 R_A.

We measured the isotopic composition of heavy noble gases in a subset of our samples, shown in Supplementary Fig. 1. Most cluster around the composition of air and ASW, though there is evidence for higher $^{84}Kr/^{36}Ar$ and $^{132}Xe/^{36}Ar$ in all samples from Rababa hot springs.

4.3. Carbon isotopes

Gases emitted from a vent in the floor of Tavurvur crater, and sampled by our UAS, range in CO_2 concentration from 432 to 555 ppm, with $\delta^{13}C$ varying from −6.48 ± 0.17 to −8.95 ± 0.03 ‰, with respect to the Pee Dee Belemnite (PDB) reference standard (Table 3, Fig. 4). We measured higher CO_2 concentrations and more positive carbon isotope compositions in fumarole gases collected on the crater rim (709 to 949 ppm CO2, −4.61 ± 0.55 to −5.39 ± 0.07 ‰) and in Rababa hot spring gases (2506 to 2646 ppm CO_2, −3.67 ± 0.06 ‰). Over the course of our one-week campaign, there was no significant temporal variation in $\delta^{13}C$ at each site. Clean air collected on a beach away from volcanic plume influence had a CO_2 concentration of 430 ppm and $\delta^{13}C$ of −7.70 ± 0.05. On a Keeling plot (Keeling, 1958), our data fall along a linear regression and the extrapolated $\delta^{13}C$ value of the pure source CO_2 is estimated to be −2.6 ± 0.62 ‰ (Fig. 4). There is no indication of degassing induced fractionation of $\delta^{13}C$, which would be predicted to result in higher $\delta^{13}C$ values in exsolved gases versus melts in both open and closed system degassing models (Barry et al., 2014; Macpherson and Mattey, 1994). Instead, variations in $\delta^{13}C$ appear to be primarily controlled by mixing between air and a source endmember (Fig. 4).

4.4. $CO_2/^3He$ values

Our samples span a range in $CO_2/^3He$ over an order of magnitude from ~2.5×10^9 to 6.7×10^{10} (Fig. 5). The minimum value is in the hot spring gases collected near Sulfur Point and lies within the MORB range of $CO_2/^3He$, 1–6 × 10^9 (Marty et al., 2020). Our samples from both Rababa hot springs and the Tavurvur crater rim fumarole are consistent

Table 2
Helium and carbon isotopes, relative abundance ratios, and estimates of mantle helium (Barry et al., 2013) and mantle (%M) and slab (limestone, %L, or sedimentary, %S) carbon (Sano and Marty, 1995) contributions from fumarole and hot spring gases sampled at Rabaul. Different noble gas isotope ratios were measured between laboratories. The 2016 Oxford uncertainty on the $^{3}He/^{4}He$ (R_C/R_A) was better than 3 %. The WHOI R_C/R_A uncertainty was better than 3.1 % in 2019 and better than 1.8 % in 2024. The UM analyses did not include $^{4}He/^{20}Ne$ and therefore were not used in calculating R_C/R_A. Not all samples were analysed for $\delta^{13}C$ ('na' signifies not analysed). ‡Samples were splits from Giggenbach bottles, all others were copper tubes. Suffix "_dup" indicates duplicate analyses of the same copper tube or Giggenbach bottle split. ¥Sampling temperatures varied across four sampled hot springs during day of sampling.

Site	Sample ID	Lab	T (°C)	R/R_A	R_C/R_A	$^{4}He/^{20}Ne$	X-value	$^{40}Ar/^{36}Ar$	$^{84}Kr/^{36}Ar$ ($\times10^{-2}$)	$^{132}Xe/^{36}Ar$ ($\times10^{-2}$)	$\delta^{13}C$	$CO_2/^{3}He$	% mantle He	% M	% L	% S
2016																
Tavurvur floor fumarole	Tav-2 A	UO	140	1.0		0.31	1.0	309.7	1.99	0.72	na	2.27×10^{8}	9			
Rababa hot spring	RB-HS-1	UO	78	6.4	6.9	3.16	9.9	320.1	4.42	3.37	−4.5	8.04×10^{9}	87	24.9	64.3	10.9
Hot spring near Sulfur Pt.	RB-HS-2	UO	82	3.3	6.2	0.46	1.5	318.6	1.68	2.31	−9.2	2.47×10^{9}	77	81.1	1.8	17.2
Garbuna crater fumarole	Gar-F-343	UO	97	7.5	7.5	36.01	113.0	307.6	3.12	2.6	na		94			
Garbuna crater fumarole	Gar-F-344	UO	89	7.1	7.2	30.71	796.4	310.0	3.82	3.53	na		90			
Silanga village hot spring	Sil-HS-345	UO	76	5.3	5.4	20.03	62.9	314.3	3.51	2.35	na		67			
Pangalu hot spring	Pan-HS-1A	UO	87	6.3	6.6	5.41	17.0	313.5	na	na	na	6.75×10^{8}	82			
Pangalu hot spring	Pan-HS-2	UO	100	2.3	6.7	3.51	11.0	312.3	3.18	2.03	−9.6	1.79×10^{9}	84			
2019																
Tavurvur rim fumarole	RB-19-1b‡	WHOI	97	1.9	5.7	0.40	1.3	na	na	na	−5.4	1.14×10^{10}	71	17.5	67.4	15.0
Tavurvur rim fumarole	RB-19-1b_dup‡	WHOI	97	2.2	6.5	0.41	1.3	na	na	na	na		81			
Tavurvur rim fumarole	RB-19-1b	UM	97	2.1		na		300.7	3.83	2.02	na					
Tavurvur rim fumarole	RB-19-1b_dup	UM	97	2.3		na		299.4	2.29	1.15	na					
Tavurvur rim fumarole	RB-19-1b2	UM	98	0.9		na		298.9	2.00	1.00	na					
Tavurvur rim fumarole	RB-19-6a‡	WHOI	98	2.7	6.0	0.48	1.5	na	na	na	−4.6	2.39×10^{10}	75	8.4	77.7	14.0
Rababa hot spring	RB-19-3a‡	WHOI	75	5.8	6.3	3.23	10.1	na	na	na	−3.7	6.71×10^{10}	79	3.0	85.3	11.7
Rababa hot spring	RB-19-3a_dup‡	WHOI	75	6.1	6.7	2.78	8.7	na	na	na	−3.7		84			
Rababa hot spring	RB-19-3a1	UM	75	5.6		na		306.3	5.36	3.06	na					
Rababa hot spring	RB-19-3a2	UM	75	6.5		na		303.7	4.84	4.63	na					
Rababa hot spring	RB-19-3a2_dup	UM	75	6.5		na		303.9	5.69	3.48	na					
2024																
Narage hot spring	P24_05-2 m-1x	WHOI	80–125¥	8.3	8.3	211.6	661.3	302.8	3.88	0.27	na					
Narage hot spring	P24_01-2 m-1x	WHOI	80–125¥	8.2		na		302.8	3.63	0.22	na					
Narage hot spring	P24_08-2 m-1x	WHOI	80–125¥	8.3	8.3	138.8	433.9	299.2	3.64	0.24	na					
Narage hot spring	P24_02-2 m-1x	WHOI	80–125¥	8.5	8.5	206.0	643.6	304.1	3.9	0.28	na					

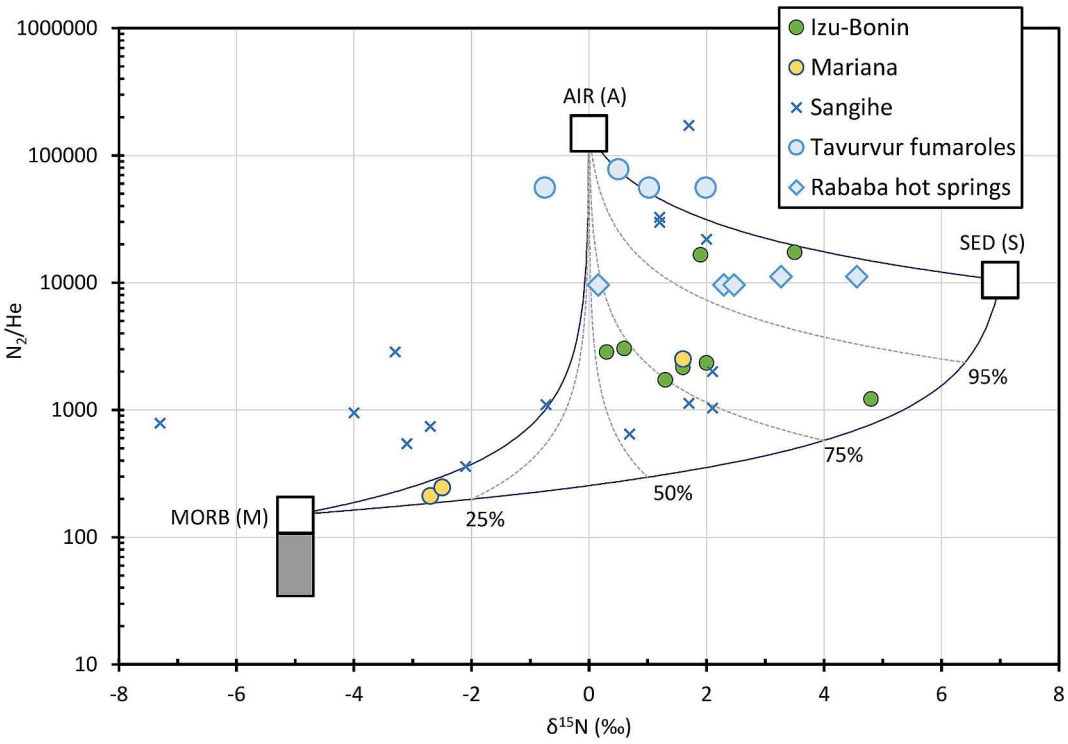

Fig. 6. N_2/He vs. $\delta^{15}N$, with mixing lines between air, sediment and mantle end members (Fischer et al., 2002; Marty and Zimmermann, 1999; Sano et al., 2001, 1998). The grey shaded field indicates the range in potential upper mantle N_2/He values (Labidi, 2022; Bekaert et al., 2021, 2023). Labelled dashed lines represent mixing (% sediment) between mantle and sediment. We also show data from other intra-oceanic arc settings, Izu-Bonin and the Northern Marianas (Mitchell et al., 2010) and Sangihe (Clor et al., 2005).

with the addition of carbon from subducted or crustal limestones. Our sample from Rababa collected in 2019 has higher $CO_2/^3He$ than the sample collected in 2016, 6.7×10^{10} compared to 8.0×10^9. All our samples lie in a region of $CO_2/^3He$ space bounded by mixing curves between MORB, subducted organic sediment and marine limestone end-members, suggesting that the carbon emitted in volcanic gases at Rabaul is partly supplied by all three of these sources. There is no indication of magma degassing processes, carbon sequestration and/or in water-gas phase fractionation processes that could potentially fractionate $CO_2/^3He$ (e.g., Barry et al., 2013; Barry et al., 2022), and thus we conclude that three component mixing best explains these data.

4.5. Nitrogen isotopes

We report nitrogen isotope data in delta notation, where $\delta^{15}N$ is the per mil (‰) deviation of the measured $^{15}N/^{14}N$ from that of air, which has $\delta^{15}N = 0$ ‰. Measured $\delta^{15}N$ ($\pm$ 1-σ errors) range from -0.75 ± 0.50 to 1.99 ± 0.80 ‰ in Tavurvur crater rim fumarole samples and from 0.16 ± 0.18 to 4.56 ± 0.63 ‰ in Rababa hot spring samples (Table 4, Fig. 6). N_2/He ranged from 55,780 to 77,835 in Tavurvur crater gases and from 9596 to 11,155 in Rababa hot spring gases. Our samples from Tavurvur crater are likely to be air contaminated (see Section 5.3). The positive enrichment in N isotopes observed in the Rababa hot springs samples is comparable to that seen in volcanic gases in other circum-Pacific arcs where nitrogen is supplied both from the mantle and from sediments carried on the subducting slab (Clor et al., 2005; Fischer et al., 2005, 2002; Mitchell et al., 2010).

5. Discussion

5.1. Atmospheric contamination

Before determining volatile provenance at Rabaul, we must first evaluate sample integrity, specifically potential contamination by atmospheric components such as air or ASW. Key indicators of substantial air contamination can include high N_2/He (43720–56,872), low He/Ar (0.002) and high O_2 (19.2–20.0 mol%), typified by our samples from Tavurvur crater floor (Table 1). Atmospheric contamination may be introduced during sample collection or, more likely, via air-saturated steam circulating in the poorly consolidated Tavurvur cone. Tavurvur rim fumarole samples, are less air contaminated, i.e., have O_2 of <0.002. All our samples fall close to either air or ASW (N_2/Ar = 80 and 43 respectively) in a N_2-He-Ar ternary diagram (Fig. 2), indicating that all are subject to variable degrees of atmospheric contamination. This is further suggested by a range in $^{40}Ar/^{36}Ar$ of 298.9–320.1, only slightly above the atmospheric value of 298.56 $\pm$ 0.31, (Lee et al., 2006). Rababa hot spring samples exhibit lower N_2/He (7267–9596) and higher $^{40}Ar/^{36}Ar$ (303.7–320.1) than Tavurvur crater rim samples (Table 1).

Helium isotopes ($^3He/^4He$) and $^4He/^{20}Ne$ (Table 2, Fig. 3) allow us a further means of evaluating variable degrees of atmospheric contamination. Tavurvur samples, both crater floor and rim, have low $^3He/^4He$ (0.9–2.7) and $^4He/^{20}Ne$ (0.3–0.4), indicating a strong atmospheric influence. Conversely, Rababa hot spring samples have higher $^3He/^4He$ (5.6–6.5 R_A) and $^4He/^{20}Ne$ (2.78–3.23), indicating less contamination. Helium isotopes can be corrected for air contamination using X-values as described in Section 4.3, though the most air contaminated samples cannot be reliably interpreted in terms of volatile sources.

Overall, on the basis of gas chemistry and He-Ne-Ar isotopes, we judge our Tavurvur (and Sulfur Point) samples to be heavily overprinted by atmospheric influence. This atmospheric contamination significantly affects gas species that are abundant in air, i.e., primarily nitrogen and therefore makes the determination of nitrogen sources in Tavurvur and Sulfur Point gases challenging. Our Rababa hot spring gases indicate a mixture of magmatic and atmospheric influence and can be used, with care, to evaluate deep volatile inputs to the Rabaul volcanic-hydrothermal system, as described below. Likewise, $\delta^{13}C$ values of our

Table 3
Carbon isotopes and measured CO_2 concentration in fumarole and hot spring gases collected in 2019. Crater floor fumaroles and clean air were sampled using a Tedlar bag onboard our multirotor UAS and analysed by Delta Ray during the fieldwork. The remaining samples were collected using Giggenbach bottles and analysed by IRMS at UNM.

Sample ID	Date	Sampling Site	CO_2 (ppm)	$\delta^{13}C$	+/−
TAV-CRF_1401	14/05/21	crater floor	467	−8.02	0.11
TAV-CRF_1402	14/05/21	crater floor	489	−7.06	0.07
TAV-CRF_1403	14/05/21	crater floor	432	−8.38	0.96
TAV-CRF_1404	14/05/21	crater floor	451	−8.54	0.58
TAV-CRF_1405	14/05/21	crater floor	443	−7.34	0.09
TAV-CRF_1601	16/05/21	crater floor	512	−7.60	0.16
TAV-CRF_1602	16/05/21	crater floor	509	−7.86	0.09
TAV-CRF_1603	16/05/21	crater floor	495	−7.94	0.06
TAV-CRF_1604	16/05/21	crater floor	454	−8.95	0.03
TAV-CRF_1605	16/05/21	crater floor	555	−7.48	0.54
TAV-CRF_1606	16/05/21	crater floor	509	−6.48	0.17
TAV-CRR_1601	16/05/21	crater rim	709	−4.61	0.55
TAV-CRR_1601	16/05/21	crater rim	949	−5.39	0.07
RB-HS1_1701	17/05/21	Rababa hot spring	2646	−3.67	0.06
RB-HS1_1702	17/05/21	Rababa hot spring	2506	−3.67	0.03
RB-AIR_1701	17/05/21	clean air	430	−7.70	0.05

gas samples from all localities extrapolate to values that are characteristic of magmatic arc fumaroles and provide information on CO_2 sources at Tavurvur.

5.2. Mantle versus crustal helium

We can use the air-corrected helium isotope composition of our samples to estimate the fraction of helium derived from the mantle and crust beneath Rabaul, assuming a binary mixture of the two end-members (Barry et al., 2013):

$$\%\text{mantle helium} = \left(R_C/R_A - {}^3He/{}^4He_{crust}\right)/\left({}^3He/{}^4He_{mantle} - {}^3He/{}^4He_{crust}\right)$$

where ${}^3He/{}^4He_{mantle} = 8\ R_A$ (Graham, 2002) and ${}^3He/{}^4He_{crust} = 0.05\ R_A$ (Morrison and Pine, 1955).

Most of our Rabaul gases are characterised by 71 to 87 % mantle helium (13 to 29 % crustal helium), with the exception of the highly air contaminated sample from the Tavurvur crater floor, which has only 10 % mantle-derived helium (Table 2). The uncertainty on our R_C/R_A estimates is 1.8–3.1 % and this can be considered the consequent uncertainty on our calculations of mantle versus crustal helium contributions. The mean (± standard deviation) of 79 ± 5 % mantle helium for our non-contaminated samples is greater than the value of 67 % mantle helium in our sample from the Sulu Range hot springs at Silanga village, and lower than the values of 82 and 84 % (Talasea) and 90 and 94 % (Garbuna) in our other New Britain volcanic gas samples (Table 2).

Mixing between primordial (mantle) and radiogenic (crustal) helium is typically controlled by crustal thickness (Barry et al., 2022; Hilton et al., 2002; Lages et al., 2021; Mason et al., 2017). Seismic refraction surveys suggest crustal thickness of ~32 km beneath Rabaul and the Gazelle Peninsula and ~ 25 km under central New Britain and the Williaumez Peninsula (Finlayson et al., 1972). Our data are consistent with a small crustal influence beneath Rabaul and a lesser influence (higher ${}^3He/{}^4He$) in central New Britain where the crust is slightly thinner, e.g., beneath the Talasea and Garbuna volcanic systems (Fig. 3). The northward increase in ${}^3He/{}^4He$, evident in our samples from Sulu, Talasea, Garbuna and Narage, peaking at >8.0 R_A, may indicate the encroaching influence of the Manus Basin plume, and is consistent with elevated ${}^3He/{}^4He$ reported in basaltic glasses from across the Manus Basin (Macpherson et al., 1998). The high ${}^3He/{}^4He$ of 8.6 R_A reported by Sano and Williams (1996) for Tavurvur was measured in gases emitted in an interval of relatively intense unrest, relative to our sampling periods, which may explain the stronger mantle/magmatic signature.

5.3. Sources of carbon

Figure 4 displays the $\delta^{13}C$ of fumarole and hot spring gases plotted against the inverse of CO_2 concentration in each sample. We also show the carbon isotope composition of reference standards, (1) limestone, that is, subducted marine carbonate ($\delta^{13}C \sim 0$ ‰) and (2) MORB, representing upper mantle material ($\delta^{13}C \sim -6.5 \pm 2.5$) (Sano and Marty, 1995). Most of our data falls on a mixing line between air and a range in $\delta^{13}C$ that is intermediate between limestone and MORB (linear correlation coefficient of 0.86, y-intercept of -2.56 ± 0.62). The range in CO_2 and $\delta^{13}C$ exhibited by our samples indicates a variable degree of mixing between ambient air and deep fumarolic hot spring gases. A sample of pristine volcanic gas, that is, without any air contamination, would plot at the far left of this mixing line, close to the y-intercept. Thus, we can estimate the carbon isotopic composition of such a gas to be $\sim -2.6 \pm 0.62$ ‰. This is isotopically high with respect to the upper mantle

Table 4
Nitrogen isotopes and estimated mantle (M), atmospheric (A) and sediment (A) percentage contributions from fumarole and hot spring gases sampled at Rabaul. M_C and S_C are percentage contributions of mantle versus sediment influence on air-corrected nitrogen isotope values, $\delta^{15}N_c$. Capital letter suffixes (A, B, C) in the sample ID column refer to separate copper tube splits of our Giggenbach bottle samples. Where present, 'dup' refers to a duplicate. Each line in the table represents the mean and standard deviation of a triplicate analysis of each copper tube split.

Site	Sample ID	Mean $\delta^{15}N$	N_2/He	% M	% A	% S	% M_C	% S_C	$\delta^{15}N_c$
2019									
Tavurvur rim fumarole	RB-19-1 A	1.02 ± 0.33	55,780	0.3	85.0	14.7	1.8	98.2	6.79
Tavurvur rim fumarole	RB-19-1C	1.99 ± 0.80	55,780	0.3	71.1	28.6	0.9	99.1	6.89
Tavurvur rim fumarole	RB-19-1b C	−0.75 ± 0.50	55,780	0.3	−10.6	110.3	−2.6	102.6	7.31
Tavurvur rim fumarole	RB-19-6a A	0.50 ± 0.53	77,835	0.2	92.6	7.2	2.6	97.4	6.69
Rababa hot spring	RB-19-3a B	0.16 ± 0.18	9596	1.6	95.0	3.4	31.6	68.4	3.21
Rababa hot spring	RB-19-3a B_dup	2.29 ± 0.42	9596	1.6	64.5	33.9	4.4	95.6	6.47
Rababa hot spring	RB-19-3a C	2.47 ± 0.56	9596	1.6	62.1	36.3	4.1	95.9	6.51
2016									
Rababa hot spring	RAB HS 1 A	4.56 ± 0.63	11,155	1.3	32.6	66.1	2.0	98.0	6.76
Rababa hot spring	RAB HS 1 B	3.27 ± 0.65	11,155	1.3	51.1	47.6	2.8	97.2	6.67

reservoir and would be consistent with CO_2 input from carbonate, either on the subducting slab or in the crustal country rocks. It closely matches the $\delta^{13}C$ values of −2.55 to −2.80 ‰ reported for Rabaul by Sano and Williams (1996).

Figure 5 displays the relative abundance of helium and CO_2 in our samples, together with their carbon isotope composition. Previous studies have established that He-CO_2 characteristics can also be used to determine relative mantle and subducted contributions (Halldórsson et al., 2013; Hilton et al., 2002; Jaffe et al., 2004; Mitchell et al., 2010; Sano and Marty, 1995; Sano and Williams, 1996; Snyder et al., 2001; van Soest et al., 1998). The method assumes that there is no crustal input of volatiles and that possible carbon reservoirs feeding volcanic outgassing are the mantle wedge (M), limestone (L) from subducted sediment or carbonate in the altered oceanic lithosphere, and sedimentary organic carbon (S). These reservoirs have distinct $CO_2/^3He$ ($M = 2 \times 10^9$, $L = 1 \times 10^{13}$, $S = 1 \times 10^{13}$) and $\delta^{13}C$ (M = −5 ‰, L = 0 ‰, S = −30 ‰) as shown in Fig. 5. Using the following equations (Sano and Marty, 1995), we can calculate the mass fraction of each potential source of carbon:

$$\left(^{13}C/^{12}C\right)_O = f_M\left(^{13}C/^{12}C\right)_M + f_L\left(^{13}C/^{12}C\right)_L + f_S\left(^{13}C/^{12}C\right)_S$$

$$1\Big/\left(^{12}C/^{3}He\right)_O = f_M\Big/\left(^{12}C/^{3}He\right)_M + f_L\left(^{12}C/^{3}He\right)_L + f_S\left(^{12}C/^{3}He\right)_S.$$

$$f_M + f_L + f_S = 1.$$

where subscripts M, L, and S correspond to the mantle, limestone and sediment end members and subscript O is the measured or observed sample.

The mean L:S:M ratio we observe in our Rabaul samples is 59:14:27, though this is subject to large standard deviation (33:3:31) owing to our sample from the hot springs near Sulfur Point plotting close to the mantle range of $\delta^{13}C$ while our remaining samples plot close to the mixing line between mantle and limestone (Fig. 5). The Sulfur Point hot springs sample is difficult to interpret: it has low $^3He/^4He$ and $^4He/^{20}Ne$ consistent with substantial air contamination, yet higher He/Ar and N_2/Ar than any of our other Rabaul samples. The mean (and standard deviation) L:S:M ratio of the four Rababa hot spring and Tavurvur crater samples is 74:13:13 (10:2:10). This composition points to a dominance of slab over mantle in supplying carbon to Rabaul and, as above, suggests carbonates are the main carbon source, with a second, more modest input from organic sediments. This is reasonable, if the subducting assemblage matches the calcareous mudstones and altered basalts sampled by dredging of the Solomon sea floor (Crook, 1986; Davies and Price, 1986). Our data from Rabaul is comparable with other intra-oceanic arcs, e.g., Sangihe (Jaffe et al., 2004) and the Antilles (van Soest et al., 1998), where carbon from slab carbonates and, to lesser extent, organic sediments is mixed into the mantle source.

Sano and Marty (1995)'s approach assumes that only the mantle and the slab supply carbon to volcanic emissions. Several studies have since argued that emissions from many volcanic arcs are subject to substantial additions of carbon via the interaction of rising magmas and crustal carbonates (Barry et al., 2022; Deegan et al., 2010; Lages et al., 2021; Mason et al., 2017; van Soest et al., 1998). Indeed, Mason et al. (2017) identify PNG (not discriminating between New Britain, West Bismarck and Bougainville) as one of a subset of arcs where outgassed carbon is sourced dominantly from crustal limestone, along with Central America, the Aegean, Indonesia, Italy and parts of the Andes. Our data suggest otherwise, with high air-corrected helium isotopes (R_C/R_A) in the majority of gas samples pointing to only minimal crustal influence on outgassing. A minor role for crustal carbon is certainly possible, given widespread growth of carbonate platforms across the region during the Miocene, but we note that these rocks are most prevalent in the western part of the Gazelle Peninsula, separated from Rabaul by major north-south trending fault systems, and may be unlikely as a result to influence the magmatic system (Lindley, 2006; Madsen and Lindley, 1994).

5.4. Sources of nitrogen

Similarly to helium and carbon, we can quantitatively resolve the different contributions to Rabaul's nitrogen output. Equations developed by (Sano et al., 1998, 2001) allow us to calculate how air (A), upper mantle (M) and sediments (S) supply nitrogen to the volcanic system using measured $\delta^{15}N$ and N_2/He values (Table 4, Fig. 6):

$$\delta^{15}N_O = \left(\delta^{15}N_A \times f_A\right) + \left(\delta^{15}N_M \times f_M\right) + \left(\delta^{15}N_S \times f_S\right).$$

$$1/\left(N_2/He\right)_O = f_A/\left(N_2/He\right)_A + f_M/\left(N_2/He\right)_M + f_S/\left(N_2/He\right)_S.$$

$$f_A + f_M + f_S = 1.$$

where f_A, f_M, and f_S are the fractions of the measured N_2 derived from air, mantle and sediment respectively and $\delta^{15}N_{A/M/S}$ and $N_2/He_{A/M/S}$ are the respective values of the end members. End member $\delta^{15}N$ values are 0 ‰ for air, −5 ± 2 ‰ for the upper mantle, and + 7 ± 4 ‰ for sediments (Sano et al., 2001). End member N_2/He values are 1.49×10^5 for air, 150 for the upper mantle, and 1.05×10^4 for sediments respectively (Fischer et al., 2002; Sano et al., 2001). We note that the N_2/He mantle end-member value of 150 cited in Fischer et al. (2002) is based on a global compilation of N-MORB glasses (Marty and Zimmermann, 1999) and that estimates based on $N_2/^3He$ (and $^3He/^4He$) in basaltic glasses and popping rocks yield lower values, ~35–122 (Bekaert et al., 2021, 2023; Javoy and Pineau, 1991; Labidi, 2022). The N_2/He value of the upper mantle does not change our following discussion substantially, given that all our samples plot far from the mantle end-member in N_2/He–$\delta^{15}N$ mixing diagrams (e.g., Fig. 6).

Recent work on nitrogen isotopologues (Labidi et al., 2021) indicates atmospheric contamination of fumarolic gases may be more extensive than can be determined from $\delta^{15}N$ and gas chemistry (e.g., N_2/Ar, N_2/He) alone. In addition, $\delta^{15}N$ values may be biased towards lower values due to kinetic isotope fractionation (Labidi et al., 2020, 2021; Labidi and Young, 2022), perhaps as a result of diffusive transport fractionation (Bekaert et al., 2023) or phase fractionation. Thus, in the absence of $^{15}N^{15}N$ data, we acknowledge that our estimates of atmospheric nitrogen contributions are likely to be minima. Our samples from Tavurvur are probably subject to the most substantial air contamination, based on air-like $\delta^{15}N$ (−0.75–1.99 ‰) and N_2/He in excess of 50,000. Our samples from Rababa show a range in $\delta^{15}N$ of 0.16–4.56 ‰ and so may provide more reliable insight into nitrogen sources. These isotopic values suggest, a degree of atmospheric influence notwithstanding, that both upper mantle and subducted organic sediments are supplying nitrogen to Rabaul's magma source region. Four of our five Rababa samples appear to be subject to only limited air contamination and contain substantial (34–66 %) sediment-derived nitrogen. Following Mitchell et al. (2010), we calculate an air-corrected nitrogen isotope composition, $\delta^{15}N_C$, that is:

$$\delta^{15}N_C = \left(\delta^{15}N_M \times f_M\right) + \left(\delta^{15}N_S \times (1 - f_M)\right).$$

where $\delta^{15}N_M = -5$ ‰, $\delta^{15}N_S = +7$ ‰ and f_M is the fraction of mantle nitrogen derived above.

We can then calculate air-corrected contributions from sediment ($S_C = S/(S + M)$) and mantle ($M_C = 1 - S_C$). For our four Rababa samples (little air contamination), S_C ranges from 96 to 98 %, pointing to a dominantly sedimentary over mantle origin for nitrogen at Rabaul. This is typical of many subduction settings, with an average of 75 % of arc nitrogen being of recycled sedimentary origin (Sano et al., 1998). There are limited data from other intra-oceanic subduction zone volcanoes to compare with Rabaul. In the Izu-Bonin-Marianas, nitrogen emissions at most volcanoes are likewise mostly of sedimentary origin, with a minor but resolvable contribution from AOC, with the exception of Agrigan

where $\delta^{15}N$ values of −2.5 to −2.7 ‰ indicate a little-modified upper mantle source (Mitchell et al., 2010). In the Sangihe arc, there is a lower sedimentary contribution to nitrogen emissions than the Sano et al. (1998) global mean of 75 %, suggesting an overall stronger influence of local upper mantle (Fig. 6). Along-arc variations in N_2/He and nitrogen isotope composition have been interpreted as variations in sediment offscraping or subducted sediment composition (Clor et al., 2005).

In summary, our $\delta^{15}N$ data, along with the $\delta^{13}C$ data described above, indicate the influence of sediment on Rabaul volatiles. On the basis of high $^3He/^4He$ in these gases, we infer that the sediment is sourced from the subducting slab and not the result of assimilation of crustal volatiles. However, nitrogen isotope data should be treated with caution due to the level of atmospheric contamination, evident in the N_2/He (Fig. 6) and the fact that N_2/Ar values are broadly air-like (Fig. 2).

5.5. Volatile provenance at Rabaul

Our data allow, for the first time, an evaluation of the origins of magmatic volatiles and therefore volcanic gases at Rabaul. Air-corrected helium isotopes, ranging from 5.7 to 6.9 R_A, are indicative of mantle-dominated helium and only minor crustal input. This is consistent with the relatively thin crust beneath Rabaul and is characteristic of most intra-oceanic arcs (Hilton et al., 2002). Gas chemistry, e.g., N_2/Ar and N_2/He, is also typical of arc volcanoes in low levels of unrest, indicating a mantle source overprinted by slab influence and a degree of atmospheric contamination (Fischer, 2008).

Carbon isotopes, with $\delta^{13}C$ of pure magmatic CO_2 (i.e., a putative air-free sample) estimated at $\sim -2.6 \pm 0.62$ ‰, suggest a mix of mantle, carbonate and organic sediment influences, with carbonate the major source (75 % in most samples). Based on our helium data, only minor volatiles can be supplied from crustal rocks and hence we suggest a limited role for decarbonation of the Miocene Yalam Formation limestones in supplying carbon to Rabaul. Instead, we favour the subducting slab as the source of both carbonate- and organic sediment-derived CO_2. The best estimates of the subducting assemblage are provided by seafloor dredging only, and we emphasise caution is required in stating that these unequivocally represent the slab lithologies. The calcareous mudrocks reported by Crook (1986) are plausible sources of both carbonate and sedimentary carbon, and the altered basalts described by Davies and Price (1986) are likely to be carbonate-bearing. Aiuppa et al. (2017) note that the Solomon Sea depth and age make it likely that the seafloor has been above the carbonate compensation depth for its entire history, which would support the idea of substantial carbonate flux into the New Britain trench on the Solomon slab.

Overall, our data support the inference made by Aiuppa et al. (2017, 2019) and subsequently by Plank and Manning (2019) that New Britain, and perhaps other arc segments in PNG, are margins where carbon emissions are dominated by recycling of subducted carbon. Further work is required to evaluate the relative importance of sedimentary carbonate versus altered ocean crust or lithosphere. Thermodynamic modelling of the New Britain subduction zone suggests that carbonate dissolution and metamorphic decarbonation of both sediments and altered basalts are necessary to explain the volcanic arc carbon flux (Arzilli et al., 2023) though we emphasise that the carbon outgassing flux presently estimated from the New Britain arc is predicted, not based on measured gas emissions (Aiuppa et al., 2019), and in our view may be biased high by the consideration only of Rabaul's emissions prior to 2014 and moreover the merging of Manam (Western Bismarck), Ulawun and Rabaul (New Britain) and Bagana (Bougainville) into the same arc segment ("PNG", see Aiuppa et al., 2017, 2019, and Plank and Manning, 2019). The thermal state of the New Britain subduction zone is neither notably hot nor cold, with a slab thermal parameter, φ, of 2510 lying slightly below (i.e., warmer) than the median value, 2994, of the global range (van Keken et al., 2011). Broadly speaking, this is likely to favour efficient devolatilization around subarc depths, rather than the pervasive shallow dewatering of the hottest slabs or the retention of volatiles beyond the arc associated with old and cold slabs (Arzilli et al., 2023; Plank and Manning, 2019; van Keken and Wilson, 2023). The modelling of van Keken et al. (2011) suggests substantial water flux from the subducting Solomon slab at depths of both 100 km and 150 km – the depth to slab below Rabaul is estimated at 148 km (Syracuse and Abers, 2006) – however the water loss trajectory for New Britain as a function of depth (see Fig. 6, van Keken et al., 2011) suggests the major pulses of slab dewatering may occur relatively before (~80–120 km) and after (~180 km). If slab partial melting is indeed important in the New Britain subduction zone (Klaver et al., 2024), this may substantially increase the efficiency of carbon recycling from the slab to the subarc mantle wedge (Plank and Manning, 2019; Poli, 2015).

Nitrogen isotopes ($\delta^{15}N$) range from 0.16 to 4.56 ‰ in our least air-contaminated (Rababa) samples, indicating the influence of a second slab phase beyond carbonate, namely sediment derived nitrogen. This fits with our carbon isotope data (i.e., highest $CO_2/^3He$ in the Rababa sample) and also the arguments advanced by Hohl et al. (2022) based on the whole-rock geochemistry and isotope composition of Rabaul lavas. Further evidence for some sediment involvement comes from our measurements of elevated $^{84}Kr/^{36}Ar$ and $^{132}Xe/^{36}Ar$ in the Rababa hot springs samples, i.e., those where heavy noble gas signatures deviate from atmospheric composition (Supplementary Fig. S1). Nitrogen isotopes in arc gases may be significantly influenced by altered ocean crust, though given a lack of constraint on the variation of $\delta^{15}N$ through the Solomon slab crust we have not attempted to evaluate this possibility quantitatively (c.f. Mitchell et al., 2010). The available nitrogen isotope data for AOC points to positive enrichments over MORB (Busigny et al., 2005, 2019; Li and Li, 2023) and it is possible that the positive $\delta^{15}N$ values of our least air-contaminated samples may also result from recycled AOC-derived nitrogen. Heterogeneity in the N_2/He content and nitrogen isotope composition of both upper mantle and slab reservoirs adds complexity to the interpretation of nitrogen source in arcs (Bekaert et al., 2021; Clor et al., 2005; Fischer et al., 2005; Labidi, 2022; Mitchell et al., 2010). Melting enhanced carbon flux from the slab may also contribute to more efficient mobilisation of nitrogen.

In summary, Rabaul volcanic gases are sourced from the mantle wedge with a substantial recycled slab overprint that supplies carbon and nitrogen from carbonates, sediments, and altered ocean crust. We anticipate that the relative proportions of slab-derived carbon versus nitrogen may be rather different, owing to different behaviours under slab metamorphism and variable derivation of each species from different slab lithologies.

6. Conclusion

We have analysed the chemical and isotopic (He-C-N-Ne-Ar-Kr-Xe) composition of fumarole and hot spring gases from Rabaul caldera, known to be among the most threatening and historically active volcanic systems in Papua New Guinea, but one where activity has declined substantially over the last decade. Ours is the first systematic study of gas composition to be undertaken at Rabaul and the first study to explore volatile provenance at this volcano. Our gas samples are subject to variable and in some cases overwhelming atmospheric contamination. Nonetheless, owing to our combination of helium (mantle versus crust), carbon (mantle versus carbonate versus organic sediments) and nitrogen (mantle versus sedimentary versus atmosphere) isotopic tracers we have been able to estimate the balance of mantle, slab, and crustal influence on Rabaul volatiles.

Rabaul gases are comparable to those of other volcanic arcs, being enriched in carbon and nitrogen. Helium isotopes point to a strong mantle rather than crustal influence, with air corrected He isotope values ranging from 5.7 to 6.9 R_A and 71–87 ± 3 % of helium in Rabaul gases originating from the mantle. Carbon isotopes ($\delta^{13}C$ estimated as −2.6 ± 0.62 ‰ for magmatic gases) indicate a combined mantle, carbonate, and organic sediment influence, with slab carbonate of either

sedimentary or altered oceanic crustal origin providing most of the carbon in Rabaul gases. Nitrogen isotopes ($\delta^{15}N \sim 0.16$–4.56 ‰ in our least air-contaminated samples) also point to a sedimentary source or potentially altered oceanic crust. We consider both carbonate and sedimentary influences to originate from the nearby subducting Solomon Sea slab, though minor contributions from arc crustal rocks are plausible, especially of carbonate.

Many characteristics of the Rabaul volcanic system remain little explored and our understanding of volatile provenance in the New Britain arc is at a nascent stage. In this contribution, our focus is to determine the reservoirs feeding outgassing from the Rabaul caldera complex, and we conclude that the nearby subducting slab plays a significant role in augmenting volatile supply from the upper mantle reservoir beneath Rabaul. Future work should investigate whether the high outgassing of the 1994–2014 eruptive interval is characteristic of the long-term behaviour of Rabaul or not, and whether Rabaul magmas are notably volatile-rich. There remain major unknowns in the wider regional geological context, including an absence of core samples of the subducting lithologies and the relative influence of both ongoing (New Britain trench) and earlier (Vitiaz-Melanesian trench) sequences of subduction recycling on the mantle wedge below the Bismarck Sea and Manus Basin.

Supplementary data to this article can be found online at https://doi.org/10.1016/j.chemgeo.2024.122434.

CRediT authorship contribution statement

B.T. McCormick Kilbride: Conceptualization, Investigation, Writing - Original Draft, Writing - Review and Editing, Visualisation, Supervision, Project Administration, Funding Acquisition. **P.H. Barry:** Conceptualization, Methodology, Investigation, Writing - Original Draft, Writing - Review and Editing, Funding Acquisition. **T. Fischer:** Conceptualization, Investigation, Methodology, **G. Holland:** Investigation, Writing - Review and Editing. **M. Hudak:** Investigation, Writing - Original Draft, Writing - Review and Editing. **S. Nowicki:** Conceptualization, Methodology, Investigation. **C. Ballentine:** Resources. **M.D. Fox:** Investigation, Funding Acquisition. **M. Höhn:** Investigation. **I. Itikarai:** Resources, Project Administration. **M. Johnson**: Investigation, Funding Acquisition. **K. Mulina:** Investigation, Project Administration. **E.J. Nicholson:** Conceptualization, Methodology, Investigation, Writing - Review and Editing, Supervision, Project Administration, Funding Acquisition.

Declaration of competing interest

The authors declare that they have no known competing financial interests or personal relationships that could have appeared to influence the work reported in this paper.

Data availability

Data will be uploaded to the EarthChem Library (https://www.earthchem.org/) following publication.

Acknowledgements

We acknowledge financial support of the Alfred P Sloan foundation, awarded via the Deep Carbon Observatory, specifically the Deep Earth Degassing (DECADE) programme of the Reservoirs and Fluxes division. BMK acknowledges a travel grant from the NERC Centre for Observation and Modelling of Earthquakes, Volcanoes and Tectonics which supported an early visit to Rabaul. PHB acknowledges NSF awards 2015789, 2121637, 2151120 and 2152551. We acknowledge a KAUST 2023 Opportunity Fund Program award to MDJ and MDF. We thank Lois Salem and Roberto D'Aleo for field assistance during the gas sampling work in 2016. We are grateful to the Tolai communities of Rabaul, especially Matupit, for their support in accessing the field sites and for valuable conversations about past and recent volcanic unrest.

References

Aiuppa, A., Fischer, T.P., Plank, T., Robidoux, P., Di Napoli, R., 2017. Along-arc, inter-arc and arc-to-arc variations in volcanic gas CO2/ST ratios reveal dual source of carbon in arc volcanism. Earth Sci. Rev. 168, 24–47. https://doi.org/10.1016/j.earscirev.2017.03.005.

Aiuppa, A., Fischer, T.P., Plank, T., Bani, P., 2019. CO2 flux emissions from the Earth's most actively degassing volcanoes, 2005–2015. Sci. Rep. 9, 5442. https://doi.org/10.1038/s41598-019-41901-y.

Andres, R., Kasgnoc, A., 1998. A time-averaged inventory of subaerial volcanic sulfur emissions. J. Geophys. Res. Atmos. 103, 25251–25261. https://doi.org/10.1029/98JD02091.

Andrews, J.N., 1985. The isotopic composition of radiogenic helium and its use to study groundwater movement in confined aquifers. Chem. Geol. Water-Rock Interact. 49, 339–351. https://doi.org/10.1016/0009-2541(85)90166-4.

Arzilli, F., Burton, M., La Spina, G., Macpherson, C.G., van Keken, P.E., McCann, J., 2023. Decarbonation of subducting carbonate-bearing sediments and basalts of altered oceanic crust: Insights into recycling of CO2 through volcanic arcs. Earth Planet. Sci. Lett. 602, 117945. https://doi.org/10.1016/j.epsl.2022.117945.

Barry, P.H., Hilton, D.R., Halldórsson, S.A., Hahm, D., Marti, K., 2012. High precision nitrogen isotope measurements in oceanic basalts using a static triple collection noble gas mass spectrometer. Geochem. Geophys. Geosyst. 13. https://doi.org/10.1029/2011GC003878.

Barry, P.H., Hilton, D.R., Fischer, T.P., de Moor, J.M., Mangasini, F., Ramirez, C., 2013. Helium and carbon isotope systematics of cold "mazuku" CO2 vents and hydrothermal gases and fluids from Rungwe Volcanic Province, southern Tanzania. Chem. Geol. Front. Gas Geochem. 339, 141–156. https://doi.org/10.1016/j.chemgeo.2012.07.003.

Barry, P.H., Hilton, D.R., Füri, E., Halldórsson, S.A., Grönvold, K., 2014. Carbon isotope and abundance systematics of Icelandic geothermal gases, fluids and subglacial basalts with implications for mantle plume-related CO2 fluxes. Geochim. Cosmochim. Acta 134, 74–99. https://doi.org/10.1016/j.gca.2014.02.038.

Barry, P.H., Lawson, M., Meurer, W.P., Warr, O., Mabry, J.C., Byrne, D.J., Ballentine, C.J., 2016. Noble gases solubility models of hydrocarbon charge mechanism in the Sleipner Vest gas field. Geochim. Cosmochim. Acta 194, 291–309. https://doi.org/10.1016/j.gca.2016.08.021.

Barry, P.H., Bekaert, D.V., Krantz, J.A., Halldórsson, S.A., de Moor, J.M., Fischer, T.P., Werner, C., Kelly, P.J., Seltzer, A.M., Franz, B.P., Kulongoski, J.T., 2021. Helium-carbon systematics of groundwaters in the Lassen Peak Region. Chem. Geol. 584, 120535. https://doi.org/10.1016/j.chemgeo.2021.120535.

Barry, P.H., De Moor, J.M., Chiodi, A., Aguilera, F., Hudak, M.R., Bekaert, D.V., Turner, S.J., Curtice, J., Seltzer, A.M., Jessen, G.L., Osses, E., Blamey, J.M., Amenábar, M.J., Selci, M., Cascone, M., Bastianoni, A., Nakagawa, M., Filipovich, R., Bustos, E., Schrenk, M.O., Buongiorno, J., Ramírez, C.J., Rogers, T.J., Lloyd, K.G., Giovannelli, D., 2022. The Helium and Carbon Isotope Characteristics of the Andean Convergent margin. Front. Earth Sci. 10.

Bekaert, D.V., Turner, S.J., Broadley, M.W., Barnes, J.D., Halldórsson, S.A., Labidi, J., Wade, J., Walowski, K.J., Barry, P.H., 2021. Subduction-Driven Volatile Recycling: a Global Mass Balance. Annu. Rev. Earth Planet. Sci. 49, 37–70. https://doi.org/10.1146/annurev-earth-071620-055024.

Bekaert, D.V., Barry, P.H., Broadley, M.W., Byrne, D.J., Marty, B., Ramírez, C.J., de Moor, J.M., Rodriguez, A., Hudak, M.R., Subhas, A.V., Halldórsson, S.A., Jessen, G.L., Blamey, J.M., Stefánsson, A., Caracausi, A., Lloyd, K.G., Giovannelli, D., Seltzer, A.M., 2023. Ultrahigh-precision noble gas isotope analyses reveal pervasive subsurface fractionation in hydrothermal systems. Sci. Adv. 9, eadg2566. https://doi.org/10.1126/sciadv.adg2566.

Bekaert, D.V., Barry, P.H., Curtice, J., Blusztajn, J., Hudak, M., Seltzer, A., Broadley, M.W., Krantz, J.A., Wanless, V.D., Soule, S.A., Mittelstaedt, E., Kurz, M.D., 2024. A carbon, nitrogen, and multi-isotope study of basalt glasses near 14°N on the Mid-Atlantic Ridge. Part a: Degassing processes. Geochim. Cosmochim. Acta 369, 160–178. https://doi.org/10.1016/j.gca.2023.12.015.

Bernard, O., Bouvet de Maisonneuve, C., 2020. Controls on eruption style at Rabaul, Papua New Guinea – Insights from microlites, porosity and permeability measurements. J. Volcanol. Geotherm. Res. 406, 107068. https://doi.org/10.1016/j.jvolgeores.2020.107068.

Bernard, O., Li, W., Costa, F., Saunders, S., Itikarai, I., Sindang, M., Bouvet de Maisonneuve, C., 2022. Explosive-effusive-explosive: the role of magma ascent rates and paths in modulating caldera eruptions. Geology 50, 1013–1017. https://doi.org/10.1130/G50023.1.

Bernstein-Taylor, B.L., Kirchoff-Stein, K.S., Silver, E.A., Reed, D.L., Mackay, M., 1992. Large-scale duplexes within the New Britain Accretionary Wedge: a possible example of accreted ophiolitic slivers. Tectonics 11, 732–752. https://doi.org/10.1029/91TC02901.

Bouvet de Maisonneuve, C., Costa, F., Patia, H., Huber, C., 2015. Mafic magma replenishment, unrest and eruption in a caldera setting: Insights from the 2006 eruption of Rabaul (Papua New Guinea). Geol. Soc. Spec. Publ. https://doi.org/10.1144/SP422.2.

Broadley, M.W., Barry, P.H., Bekaert, D.V., Byrne, D.J., Caracausi, A., Ballentine, C.J., Marty, B., 2020. Identification of chondritic krypton and xenon in Yellowstone gases and the timing of terrestrial volatile accretion. Proc. Natl. Acad. Sci. 117, 13997–14004. https://doi.org/10.1073/pnas.2003907117.

Busigny, V., Laverne, C., Bonifacie, M., 2005. Nitrogen content and isotopic composition of oceanic crust at a superfast spreading ridge: a profile in altered basalts from ODP Site 1256, Leg 206. Geochem. Geophys. Geosyst. 6. https://doi.org/10.1029/2005GC001020.

Busigny, V., Cartigny, P., Laverne, C., Teagle, D., Bonifacie, M., Agrinier, P., 2019. A re-assessment of the nitrogen geochemical behavior in upper oceanic crust from Hole 504B: Implications for subduction budget in Central America. Earth Planet. Sci. Lett. 525. https://doi.org/10.1016/j.epsl.2019.115735.

Carn, S.A., Clarisse, L., Prata, A.J., 2016. Multi-decadal satellite measurements of global volcanic degassing. J. Volcanol. Geotherm. Res. 311, 99–134. https://doi.org/10.1016/j.jvolgeores.2016.01.002.

Carn, S.A., Fioletov, V.E., McLinden, C.A., Li, C., Krotkov, N.A., 2017. A decade of global volcanic SO2 emissions measured from space. Sci. Rep. 7, 44095. https://doi.org/10.1038/srep44095.

Clor, L.E., Fischer, T.P., Hilton, D.R., Sharp, Z.D., Hartono, U., 2005. Volatile and N isotope chemistry of the Molucca Sea collision zone: Tracing source components along the Sangihe Arc, Indonesia. Geochem. Geophys. Geosyst. 6. https://doi.org/10.1029/2004GC000825.

Craig, H., Poreda, R.J., 1987. Studies of methane and helium in hydrothermal vent plumes, spreading-axis basalts and volcanic island lavas and gases in Southwest Pacific marginal basins. Scripps Ins. Oceanogr.

Crook, K.A.W., 1986. Petrology and mineral chemistry of sedimentary rocks from the Western Solomon Sea. Geo-Mar. Lett. 6, 203–209. https://doi.org/10.1007/BF02239581.

Davies, H.L., Price, R.C., 1986. Basalts from the Solomon and Bismarck Seas. Geo-Mar. Lett. 6, 193–202. https://doi.org/10.1007/BF02239580.

Deegan, F.M., Troll, V.R., Freda, C., Misiti, V., Chadwick, J.P., McLeod, C.L., Davidson, J. P., 2010. Magma–Carbonate interaction processes and associated CO2 release at Merapi Volcano, Indonesia: insights from experimental petrology. J. Petrol. 51, 1027–1051. https://doi.org/10.1093/petrology/egq010.

DePaolo, D.J., Johnson, R.W., 1979. Magma genesis in the New Britain island-arc: Constraints from Nd and Sr isotopes and trace-element patterns. Contrib. Mineral. Petrol. 70, 367–379. https://doi.org/10.1007/BF00371044.

Fabbro, G.N., McKee, C.O., Sindang, M.E., Eggins, S., Bouvet de Maisonneuve, C., 2020. Variable mafic recharge across a caldera cycle at Rabaul, Papua New Guinea. J. Volcanol. Geotherm. Res. 393, 106810. https://doi.org/10.1016/j.jvolgeores.2020.106810.

Farley, K.A., Patterson, D., McInnes, B., 1995. He-isotopic investigation of geothermal gases from the Tabar-Lihir-Tanga-Feni arc and Rabaul, Papua New Guinea. AIP Conf. Proc. 341, 81–90. https://doi.org/10.1063/1.48752.

Finlayson, D.M., Cull, J.P., Wiebenga, W.A., Furumoto, A.S., Webb, J.P., 1972. New Britain—New Ireland Crustal Seismic Refraction Investigations 1967 and 1969. Geophys. J. Int. 29, 245–253. https://doi.org/10.1111/j.1365-246X.1972.tb06157.x.

Fischer, T.P., 2008. Fluxes of volatiles (H_2O, CO_2, N_2, Cl, F) from arc volcanoes. Geochem. J. 42, 21–38. https://doi.org/10.2343/geochemj.42.21.

Fischer, T.P., Lopez, T.M., 2016. First airborne samples of a volcanic plume for δ13C of CO2 determinations. Geophys. Res. Lett. 43, 3272–3279. https://doi.org/10.1002/2016GL068499.

Fischer, T.P., Giggenbach, W.F., Sano, Y., Williams, S.N., 1998. Fluxes and sources of volatiles discharged from Kudryavy, a subduction zone volcano, Kurile Islands. Earth Planet. Sci. Lett. 160, 81–96. https://doi.org/10.1016/S0012-821X(98)00086-7.

Fischer, T.P., Hilton, D.R., Zimmer, M.M., Shaw, A.M., Sharp, Z.D., Walker, J.A., 2002. Subduction and Recycling of Nitrogen along the central American margin. Science 297, 1154–1157. https://doi.org/10.1126/science.1073995.

Fischer, T.P., Takahata, N., Sano, Y., Sumino, H., Hilton, D.R., 2005. Nitrogen isotopes of the mantle: Insights from mineral separates. Geophys. Res. Lett. 32, 1–5. https://doi.org/10.1029/2005GL022792.

Fischer, T.P., Arellano, S., Carn, S., Aiuppa, A., Galle, B., Allard, P., Lopez, T., Shinohara, H., Kelly, P., Werner, C., Cardellini, C., Chiodini, G., 2019. The emissions of CO2 and other volatiles from the world's subaerial volcanoes. Sci. Rep. 9, 18716. https://doi.org/10.1038/s41598-019-54682-1.

Fischer, T.P., Lopez, T.M., Aiuppa, A., Rizzo, A.L., Ilanko, T., Kelley, K.A., Cottrell, E., 2021. Gas Emissions from the Western Aleutians Volcanic Arc. Front. Earth Sci. 9.

Galewsky, J., Silver, E.A., 1997. Tectonic controls on facies transitions in an oblique collision: the western Solomon Sea, Papua New Guinea. GSA Bull. 109, 1266–1278. https://doi.org/10.1130/0016-7606(1997)109<1266:TCOFTI>2.3.CO;2.

Galle, B., Arellano, S., Bobrowski, N., Conde, V., Fischer, T.P., Gerdes, G., Gutmann, A., Hoffmann, T., Itikarai, I., Krejci, T., Liu, E.J., Mulina, K., Nowicki, S., Richardson, T., Rüdiger, J., Wood, K., Xu, J., 2021. A multi-purpose, multi-rotor drone system for long-range and high-altitude volcanic gas plume measurements. Atmos. Meas. Tech. 14, 4255–4277. https://doi.org/10.5194/amt-14-4255-2021.

Giggenbach, W.F., 1975. A simple method for the collection and analysis of volcanic gas samples. Bull. Volcanol. 39, 132–145. https://doi.org/10.1007/BF02596953.

Giggenbach, W., 1980. Geothermal gas equilibria. Geochimica Cosmochimica Acta 44 (12), 2021–2032.

Giggenbach, W.F., Goguel, R.L., 1989. Methods for the Collection and Analysis of Geothermal and Volcanic Water and Gas Samples. Chemistry Division, Department of Scientific and Industrial Research.

Global Volcanism Program, 1995. Report on Rabaul (Papua New Guinea) — December 1995. Bull. Glob. Volcan. Netw. 20.

Global Volcanism Program, 1997a. Global Volcanism Program | Report on Rabaul (Papua New Guinea) — November 1997 22.

Global Volcanism Program, 1997b. Global Volcanism Program | Report on Rabaul (Papua New Guinea) — December 1997 22.

Global Volcanism Program, 2013. Volcanoes of the World [WWW Document]. V 4110 08 Jun 2022. URL. https://volcano.si.edu/ (accessed 6.30.22).

Gong, W., Xing, J., Xu, C., Zhang, H., Liu, Y., Chen, W., 2023. Heterogeneous morphology of the Solomon Sea slab along the New Britain Trench and its dynamic implications from the analysis of seismicity and gravity anomalies. Geol. J. 58, 1–20. https://doi.org/10.1002/gj.4578.

Graham, D.W., 2002. Noble Gas Isotope Geochemistry of Mid-Ocean Ridge and Ocean Island Basalts: Characterization of Mantle Source Reservoirs. Rev. Mineral. Geochem. 47, 247–317. https://doi.org/10.2138/rmg.2002.47.8.

Halldórsson, S.A., Hilton, D.R., Troll, V.R., Fischer, T.P., 2013. Resolving volatile sources along the western Sunda arc, Indonesia. Chem. Geol. 339, 263–282. https://doi.org/10.1016/j.chemgeo.2012.09.042.

Heming, R.F., 1974. Geology and petrology of Rabaul Caldera, Papua New Guinea. Bull. Geol. Soc. Am. 85, 1253–1264. https://doi.org/10.1130/0016-7606(1974)85<1253:GAPORC>2.0.CO;2.

Hilton, D.R., 1996. The helium and carbon isotope systematics of a continental geothermal system: results from monitoring studies at Long Valley caldera (California, U.S.a.). Chem. Geol. 127, 269–295. https://doi.org/10.1016/0009-2541(95)00134-4.

Hilton, D.R., Fischer, T.P., Marty, B., 2002. Noble gases and Volatile Recycling at Subduction zones. Rev. Mineral. Geochem. 47, 319–370. https://doi.org/10.2138/rmg.2002.47.9.

Hohl, S.V., Schuth, S., Münker, C., König, S., Garbe-Schönberg, D., Kuduon, J., 2022. Geochemical evolution of the Rabaul volcanic complex, Papua New Guinea - Insights from HFSE, Sr-Nd-Hf, and Fe isotopes. Lithos 408–409, 106560. https://doi.org/10.1016/j.lithos.2021.106560.

Holm, R.J., Rosenbaum, G., Richards, S.W., 2016. Post 8Ma reconstruction of Papua New Guinea and Solomon Islands: Microplate tectonics in a convergent plate boundary setting. Earth Sci. Rev. 156, 66–81. https://doi.org/10.1016/j.earscirev.2016.03.005.

Honza, E., Miyazaki, T., Lock, J., 1989. Subduction erosion and accretion in the Solomon Sea region. Tectonophys. Subduct. Zones: Kaiko Proj. 160, 49–62. https://doi.org/10.1016/0040-1951(89)90383-1.

Ilanko, T., Fischer, T.P., Kyle, P., Curtis, A., Lee, H., Sano, Y., 2019. Modification of fumarolic gases by the ice-covered edifice of Erebus volcano, Antarctica. J. Volcanol. Geotherm. Res. 381, 119–139. https://doi.org/10.1016/j.jvolgeores.2019.05.017.

Jaffe, L.A., Hilton, D.R., Fischer, T.P., Hartono, U., 2004. Tracing magma sources in an arc-arc collision zone: Helium and carbon isotope and relative abundance systematics of the Sangihe Arc, Indonesia. Geochem. Geophys. Geosyst. 5. https://doi.org/10.1029/2003GC000660.

Jambon, A., 1994. Earth degassing and large-scale geochemical cycling of volatile elements. Rev. Mineral. Geochem. 30, 479–517.

Javoy, M., Pineau, F., 1991. The volatiles record of a "popping" rock from the Mid-Atlantic Ridge at 14°N: chemical and isotopic composition of gas trapped in the vesicles. Earth Planet. Sci. Lett. 107, 598–611. https://doi.org/10.1016/0012-821X(91)90104-P.

Johnson, R.W., 1979. Geotectonics and volcanism in Papua New Guinea: a review of the late Cainozoic. BMR J. Aust. Geol. Geophys. 4, 181–207.

Johnson, R.W., McKee, C.O., Eggins, S., Woodhead, J.D., Arculus, R.J., Chappell, B.W., Sheraton, J., 1995. Taking petrologic pathways toward understanding Rabaul's restless caldera. EOS Trans. Am. Geophys. Union 76, 171–180. https://doi.org/10.1029/95EO00093.

Joshima, M., Honza, E., 1986. Age estimation of the Solomon Sea based on heat flow data. Geo-Mar. Lett. 6, 211–217. https://doi.org/10.1007/BF02239582.

Joshima, M., Okuda, Y., Murakami, F., Kishimoto, K., Honza, E., 1986. Age of the Solomon Sea Basin from magnetic lineations. Geo-Mar. Lett. 6, 229–234. https://doi.org/10.1007/BF02239584.

Kagoshima, T., Sano, Y., Takahata, N., Maruoka, T., Fischer, T.P., Hattori, K., 2015. Sulphur geodynamic cycle. Sci. Rep. 5, 8330. https://doi.org/10.1038/srep08330.

Keeling, C.D., 1958. The concentration and isotopic abundances of atmospheric carbon dioxide in rural areas. Geochim. Cosmochim. Acta 13, 322–334. https://doi.org/10.1016/0016-7037(58)90033-4.

van Keken, P.E., Wilson, C.R., 2023. An introductory review of the thermal structure of subduction zones: III—Comparison between models and observations. Prog. Earth Planet Sci. 10, 57. https://doi.org/10.1186/s40645-023-00589-5.

van Keken, P.E., Hacker, B.R., Syracuse, E.M., Abers, G.A., 2011. Subduction factory: 4. Depth-dependent flux of H2O from subducting slabs worldwide. J. Geophys. Res. Solid Earth 116. https://doi.org/10.1029/2010JB007922.

Klaver, M., Yogodzinski, G., Albert, C., Camejo-Harry, M., Elburg, M., Hoernle, K., Macpherson, C., Nowell, G., Rushmer, T., Williams, H., Millet, M.-A., 2024. Widespread slab melting in modern subduction zones. Earth Planet. Sci. Lett. 626, 118544. https://doi.org/10.1016/j.epsl.2023.118544.

Labidi, J., 2022. The origin of nitrogen in Earth's mantle: Constraints from basalts 15N/14N and N2/3He ratios. Chem. Geol. 597, 120780. https://doi.org/10.1016/j.chemgeo.2022.120780.

Labidi, J., Young, E.D., 2022. The origin and dynamics of nitrogen in the Earth's mantle constrained by 15N15N in hydrothermal gases. Chem. Geol. 591, 120709. https://doi.org/10.1016/j.chemgeo.2022.120709.

Labidi, J., Barry, P.H., Bekaert, D.V., Broadley, M.W., Marty, B., Giunta, T., Warr, O., Sherwood Lollar, B., Fischer, T.P., Avice, G., Caracausi, A., Ballentine, C.J., Halldórsson, S.A., Stefánsson, A., Kurz, M.D., Kohl, I.E., Young, E.D., 2020. Hydrothermal 15N15N abundances constrain the origins of mantle nitrogen. Nature 580, 367–371. https://doi.org/10.1038/s41586-020-2173-4.

Labidi, J., Young, E.D., Fischer, T.P., Barry, P.H., Ballentine, C.J., de Moor, J.M., 2021. Recycling of nitrogen and light noble gases in the central American subduction zone:

Constraints from 15N15N. Earth Planet. Sci. Lett. 571, 117112. https://doi.org/10.1016/j.epsl.2021.117112.
Lages, J., Rizzo, A.L., Aiuppa, A., Samaniego, P., Le Pennec, J.L., Ceballos, J.A., Narváez, P.A., Moussallam, Y., Bani, P., Schipper, C.I., Hidalgo, S., Gaglio, V., Alberti, E., Sandoval-Velasquez, A., 2021. Noble gas magmatic signature of the Andean Northern Volcanic Zone from fluid inclusions in minerals. Chem. Geol. 559, 119966. https://doi.org/10.1016/j.chemgeo.2020.119966.
Leat, P.T., Larter, R.D., 2003. Intra-oceanic subduction systems: introduction. Geol. Soc. Lond. Spec. Publ. 219, 1–17. https://doi.org/10.1144/GSL.SP.2003.219.01.01.
Lee, H., Fischer, T.P., Muirhead, J.D., Ebinger, C.J., Kattenhorn, S.A., Sharp, Z.D., Kianji, G., Takahata, N., Sano, Y., 2017. Incipient rifting accompanied by the release of subcontinental lithospheric mantle volatiles in the Magadi and Natron basin, East Africa. J. Volcanol. Geotherm. Res. Volcano-Hydrother. Syst. 346, 118–133. https://doi.org/10.1016/j.jvolgeores.2017.03.017.
Lee, J.-Y., Marti, K., Severinghaus, J.P., Kawamura, K., Yoo, H.-S., Lee, J.B., Kim, J.S., 2006. A redetermination of the isotopic abundances of atmospheric Ar. Geochim. Cosmochim. Acta 70, 4507–4512. https://doi.org/10.1016/j.gca.2006.06.1563.
Li, K., Li, L., 2023. Nitrogen enrichment in the altered upper oceanic crust: a new perspective on constraining the global subducting nitrogen budget and implications for subduction-zone nitrogen recycling. Earth Planet. Sci. Lett. 602, 117960. https://doi.org/10.1016/j.epsl.2022.117960.
Lindley, I., 2006. Extensional and vertical tectonics in the New Guinea islands: implications for island arc evolution. Ann. Geophys. 49.
Liu, E.J., Aiuppa, A., Alan, A., Arellano, S., Bitetto, M., Bobrowski, N., Carn, S., Clarke, R., Corrales, E., de Moor, J.M., Diaz, J.A., Edmonds, M., Fischer, T.P., Freer, J., Fricke, G.M., Galle, B., Gerdes, G., Giudice, G., Gutmann, A., Hayer, C., Itikarai, I., Jones, J., Mason, E., McCormick Kilbride, B.T., Mulina, K., Nowicki, S., Rahilly, K., Richardson, T., Rüdiger, J., Schipper, C.I., Watson, I.M., Wood, K., 2020. Aerial strategies advance volcanic gas measurements at inaccessible, strongly degassing volcanoes. Sci. Adv. 6, eabb9103. https://doi.org/10.1126/sciadv.abb9103.
Macpherson, C., Mattey, D., 1994. Carbon isotope variations of CO2 in Central Lau Basin basalts and ferrobasalts. Earth Planet. Sci. Lett. 121, 263–276. https://doi.org/10.1016/0012-821X(94)90072-8.
Macpherson, C.G., Hilton, D.R., Sinton, J.M., Poreda, R.J., Craig, H., 1998. High 3He/4He ratios in the Manus backarc basin: Implications for mantle mixing and the origin of plumes in the western Pacific Ocean. Geology 26, 1007–1010. https://doi.org/10.1130/0091-7613(1998)026<1007:HHHRIT>2.3.CO;2.
Madsen, J.A., Lindley, I.D., 1994. Large-scale structures on Gazelle Peninsula, New Britain: Implications for the evolution of the New Britain arc. Aust. J. Earth Sci. 41, 561–569. https://doi.org/10.1080/08120099408728166.
Malatesta, C., Gerya, T., Crispini, L., Federico, L., Capponi, G., 2013. Oblique subduction modelling indicates along-trench tectonic transport of sediments. Nat. Commun. 4, 2456. https://doi.org/10.1038/ncomms3456.
Marty, B., Zimmermann, L., 1999. Volatiles (he, C, N, Ar) in mid-ocean ridge basalts: assessment of shallow-level fractionation and characterization of source composition. Geochim. Cosmochim. Acta 63, 3619–3633. https://doi.org/10.1016/S0016-7037(99)00169-6.
Marty, B., Almayrac, M., Barry, P.H., Bekaert, D.V., Broadley, M.W., Byrne, D.J., Ballentine, C.J., Caracausi, A., 2020. An evaluation of the C/N ratio of the mantle from natural CO2-rich gas analysis: Geochemical and cosmochemical implications. Earth Planet. Sci. Lett. 551, 116574. https://doi.org/10.1016/j.epsl.2020.116574.
Mason, E., Edmonds, M., Turchyn, A.V., 2017. Remobilization of crustal carbon may dominate volcanic arc emissions. Science 357, 290–294. https://doi.org/10.1126/science.aan5049.
McCormick, B.T., Edmonds, M., Mather, T.A., Carn, S.A., 2012. First synoptic analysis of volcanic degassing in Papua New Guinea. Geochem. Geophys. Geosyst. 13. https://doi.org/10.1029/2011GC003945.
McCormick Kilbride, B.T., Nicholson, E.J., Wood, K.T., Wilkes, T.C.S., Schipper, C.I., Mulina, K., Itikarai, I., Richardson, T., Werner, C., Hayer, C.S.L., Esse, B., Burton, M., Pering, T.D., McGonigle, A.J.S., Coppola, D., Bitetto, M., Giudice, G., Aiuppa, A., 2023. Temporal Variability in Gas Emissions at Bagana Volcano Revealed by Aerial, Ground, and Satellite Observations. Geochem. Geophys. Geosyst. 24 (6), e2022GC010786.
McGonigle, A.J.S., Oppenheimer, C., Tsanev, V.I., Saunders, S., Mulina, K., Tohui, S., Bosco, J., Nahou, J., Kuduon, J., Taranu, F., 2004. Sulphur dioxide fluxes from Papua New Guinea's volcanoes. Geophys. Res. Lett. 31. https://doi.org/10.1029/2004GL019568.
McKee, C.O., 2015. Tavui Volcano: neighbour of Rabaul and likely source of the Middle Holocene penultimate major eruption in the Rabaul area. Bull. Volcanol. 77. https://doi.org/10.1007/s00445-015-0968-1.
McKee, C.O., Duncan, R.A., 2016. Early volcanic history of the Rabaul area. Bull. Volcanol. 78. https://doi.org/10.1007/s00445-016-1018-3.
McKee, C.O., Baillie, M.G., Reimer, P.J., 2015. A revised age of ad 667–699 for the latest major eruption at Rabaul. Bull. Volcanol. 77. https://doi.org/10.1007/s00445-015-0954-7.
Mitchell, E.C., Fischer, T.P., Hilton, D.R., Hauri, E.H., Shaw, A.M., De Moor, J.M., Sharp, Z.D., Kazahaya, K., 2010. Nitrogen sources and recycling at subduction zones: Insights from the Izu-Bonin-Mariana arc. Geochem. Geophys. Geosyst. 11. https://doi.org/10.1029/2009GC002783.
Morris, J.D., Leeman, W.P., Tera, F., 1990. The subducted component in island arc lavas: constraints from Be isotopes and B–Be systematics. Nature 344, 31–36. https://doi.org/10.1038/344031a0.
Morrison, P., Pine, J., 1955. Radiogenic Origin of the Helium Isotopes in Rock. Ann. N. Y. Acad. Sci. 62, 71–92. https://doi.org/10.1111/j.1749-6632.1955.tb35366.x.
Nairn, I.A., Mckee, C.O., Talai, B., Wood, C.P., 1995. Geology and eruptive history of the Rabaul Caldera area, Papua New Guinea. J. Volcanol. Geotherm. Res. 69, 255–284. https://doi.org/10.1016/0377-0273(95)00035-6.
Ozima, M., Podosek, F.A., 2002. Noble gas Geochemistry, 2nd ed. Cambridge University Press, Cambridge. https://doi.org/10.1017/CBO9780511545986.
Patia, H., Eggins, S.M., Arculus, R.J., McKee, C.O., Johnson, R.W., Bradney, A., 2017. The 1994–2001 eruptive period at Rabaul, Papua New Guinea: Petrological and geochemical evidence for basalt injections into a shallow dacite magma reservoir, and significant SO2 flux. J. Volcanol. Geotherm. Res. 345, 200–217. https://doi.org/10.1016/j.jvolgeores.2017.08.011.
Plank, T., Manning, C.E., 2019. Subducting carbon. Nature 574, 343–352. https://doi.org/10.1038/s41586-019-1643-z.
Poli, S., 2015. Carbon mobilized at shallow depths in subduction zones by carbonatitic liquids. Nat. Geosci. 8, 633–636. https://doi.org/10.1038/ngeo2464.
Sano, Y., Marty, B., 1995. Origin of carbon in fumarolic gas from island arcs. Chem. Geol. 119, 265–274. https://doi.org/10.1016/0009-2541(94)00097-R.
Sano, Y., Williams, S.N., 1996. Fluxes of mantle and subducted carbon along convergent plate boundaries. Geophys. Res. Lett. 23, 2749–2752. https://doi.org/10.1029/96GL02260.
Sano, Y., Takahata, N., Nishio, Y., Marty, B., 1998. Nitrogen recycling in subduction zones. Geophys. Res. Lett. 25, 2289–2292. https://doi.org/10.1029/98GL01687.
Sano, Y., Takahata, N., Nishio, Y., Fischer, T.P., Williams, S.N., 2001. Volcanic flux of nitrogen from the Earth. Chem. Geol. 171, 263–271. https://doi.org/10.1016/S0009-2541(00)00252-7.
Snyder, G., Poreda, R., Hunt, A., Fehn, U., 2001. Regional variations in volatile composition: Isotopic evidence for carbonate recycling in the central American volcanic arc. Geochem. Geophys. Geosyst. 2. https://doi.org/10.1029/2001GC000163.
van Soest, M.C., Hilton, D.R., Kreulen, R., 1998. Tracing crustal and slab contributions to arc magmatism in the lesser antilles island arc using helium and carbon relationships in geothermal fluids. Geochim. Cosmochim. Acta 62, 3323–3335. https://doi.org/10.1016/S0016-7037(98)00241-5.
Syracuse, E.M., Abers, G.A., 2006. Global compilation of variations in slab depth beneath arc volcanoes and implications. Geochem. Geophys. Geosyst. 7. https://doi.org/10.1029/2005GC001045.
Tregoning, P., Lambeck, K., Stolz, A., Morgan, P., McClusky, S.C., van der Beek, P., McQueen, H., Jackson, R.J., Little, R.P., Laing, A., Murphy, B., 1998. Estimation of current plate motions in Papua New Guinea from Global Positioning System observations. J. Geophys. Res. Solid Earth 103, 12181–12203. https://doi.org/10.1029/97JB03676.
Tregoning, P., McQueen, H., Lambeck, K., Jackson, R., Little, R., Saunders, S., Rosa, R., 2000. Present-day crustal motion in Papua New Guinea. Earth Planets Space 52, 727–730. https://doi.org/10.1186/BF03352272.
Wood, C.P., Nairn, I.A., Mckee, C.O., Talai, B., 1995. Petrology of the Rabaul Caldera area, Papua New Guinea. J. Volcanol. Geotherm. Res. 69, 285–302. https://doi.org/10.1016/0377-0273(95)00034-8.
Woodhead, J.D., Johnson, R.W., 1993. Isotopic and trace-element profiles across the New Britain island arc, Papua New Guinea. Contrib. Mineral. Petrol. 113, 479–491. https://doi.org/10.1007/BF00698317.
Woodhead, J.D., Eggins, S.M., Johnson, R.W., 1998. Magma Genesis in the New Britain Island Arc: further Insights into Melting and Mass transfer Processes. J. Petrol. 39, 1641–1668. https://doi.org/10.1093/petroj/39.9.1641.
Zhang, H., Gong, W., Xing, J., Xu, C., Li, C., 2023. The Subduction Structure beneath the New Britain Island Arc and the Adjacent Region from Double-Difference Tomography. J. Ocean Univ. China 22, 107–118. https://doi.org/10.1007/s11802-023-5282-5.